Per. Mineral. (2003), *72*, SPECIAL ISSUE: *Miocene to Recent...*, **73-104** http://go.to/permin

PERIODICO di MINERALOGIA
established in 1930

An International Journal of
MINERALOGY, CRYSTALLOGRAPHY, GEOCHEMISTRY, ORE DEPOSITS, PETROLOGY, VOLCANOLOGY
and applied topics on *Environment, Archaeometry* and *Cultural Heritage*

CHAPTER 2
Elba Island: intrusive magmatism

SERGIO ROCCHI[1]*, ANDREA DINI[2], FABRIZIO INNOCENTI[1], SONIA TONARINI[2] and DAVID S. WESTERMAN[3]

[1] Dipartimento di Scienze della Terra, Università di Pisa, Via S. Maria, 53, Pisa, 56126, Italy
[2] CNR, Istituto di Geoscienze e Georisorse, Via Moruzzi, 1, 56124, Pisa, Italy
[3] Norwich University, Department of Geology, Northfield, Vermont 05663, USA

2.1 HISTORICAL PERSPECTIVE

The first inhabitants of Elba Island were Musterian/Neanderthal men, about 50,000 years ago. At that time, during the Würm glaciation, the sea level was some 100 m lower, and it was possible to walk from mainland Tuscany to Elba, Gorgona, Capraia, Montecristo and Pianosa islands. About 18,000 years ago, individuals of Homo Sapiens were living in Elba. Some 12,000 years ago the isthmus joining the Elba to Tuscany was submerged, but no people remained in Elba. During the Neolithic, some 5,000 years B.C., people came again to Elba, and 2,000 years ago they started to exploit the copper ores from ophiolitic sequences of western, central and eastern Elba. Thus, Elba Island, with its potential of iron ores, joined the history of the main Mediterranean civilisations and is reported in the legend of Jason and the Argonauts. During the VIII century B.C. the Etruscans with their king, Tyrrhenus, arrived in Tuscany. At around 650 B.C., when the wars in the Middle East discontinued the iron supply from the Anatolian region to the Mediterranean area, the Etruscan mines of Elba Island and southern Tuscany became the major producers of iron and other metals such as copper, lead, zinc, silver. Aristotle refers to Elba when he speaks about a little island in the Etruscan region where metals, such as iron and copper, were mined, and he calls this island «Aethalia» (i.e. sooty) owing to the smoke from smelting furnaces.

At the beginning of the fourth century B.C., the Greeks coming from Siracusa conquered Elba. About a century later, the Romans took control of the island and exploited its iron ores. Their techniques were rough, leaving up to 70% of the iron in the scoria, while the Etruscans had been able to extract twice this quantity. Moreover, the Romans almost completely destroyed the woods of Elba to supply their furnaces, whereas Etruscans cut the trees according to their age. Then, during the II century B.C., the Romans started to take metal from Sardinia, Spain, Germany and France. Finally, during the I century B.C., the Romans finally swept the threat of the pirates out of the Mediterranean Sea and proudly called it Mare Nostrum (i.e. Our Sea). At this time, Romans built beautiful villas on the islands of the Tuscan Archipelago, and the first Emperor, Augustus, established that no more trees could be cut on Elba to supply furnaces. The Romans started to quarry the granite of western Elba, and columns from there can be admired today at the Pantheon and Saint Paul's cathedral in Rome. At this time Plinius and Virgil referred to the island as «Ilva», a name deriving from a people coming from Ligury and living in Elba.

* Corresponding author, E-mail: rocchi@dst.unipi.it

The documented history of Elba begins with Christianity and the Middle Ages, and the name «Elba» was first used by Pope Gregorius Magnus. In the eleventh century, Elba became a possession of the Republic of Pisa, who started to exploit the iron ores again and defended the island against the Saracen pirates with mountain- and sea-towers, fortresses (Volterraio and Marciana) and churches. From the end of the XIII century to the French Revolution, Elba Island was dominated by ever changing powers, i.e. Genoa, Spain, the Medici of Florence, the Lorraines of Tuscany, the Bourbons of Naples. During the years of Napoleon's wars, Elba Island suffered complex events, and finally, after the defeat of Lipsia, Napoleon arrived in exile at Elba on May 1814. He built streets, set down administrative rules, supported the public health, and imposed a new development of the mining industry. On February 26, 1815, Napoleon left the island with 1100 followers taking advantage of the absence of the English Commissioner. He would never come back, but Elba will never forget him. He left here his two residences, a town house, Villa dei Mulini, and a country house, Villa San Martino.

After Napoleon's departure and his defeat, Elba was annexed to the Grand Duchy of Tuscany in 1815 and it became part of the newly born Italy by plebiscite in 1860. The Italian Elba became an important iron centre and it went through a flourishing trade development that also brought a stream of immigrants from the mainland. This industrial development was also favoured by the loss of excessive bureaucracy due to the unification of Italy. Yet, a new threat was already hanging over Elba, and the outbreak of the World War II caused the destruction of Portoferraio. In the post-war period the island started up its tourist trade, leaving forever the industrial activities.

2.2 GEOLOGIC SETTING

2.2.1 Regional geology

Elba Island is located at the northern end of the Tyrrhenian Sea, a region affected by extensional processes behind the eastward migrating compressive regime in the hanging wall of the eastward retreating Apennine slab (Malinverno and Ryan, 1986; Fig. 1). The backbone structure of the Apennine mobile belt was constructed during an early Miocene compressive phase in the collision zone between the Sardinia-Corsica block and the Adria plate (Keller and Pialli, 1990). This orogenic system evolved diachronously as the regime of extension migrated from west to east, trailing the retreat of the compressive regime (Brunet *et al.*, 2000) and giving way to the opening of the Tyrrhenian basin. In this framework, magmas were generated in the mantle and interacted with crust-derived felsic magmas to generate the variety of Tuscan Magmatic Province intrusive and extrusive products exposed over about 30,000 km^2 of southern Tuscany and the northern Tyrrhenian Sea (Juteau at al., 1986; Giraud *et al.*, 1986; Ferrara *et al.*, 1989; Poli *et al.*, 1989; Pinarelli, 1991; Poli, 1992; Innocenti *et al.*, 1992; Innocenti *et al.*, 1997; Westerman *et al.*, 1993). This igneous activity migrated from west (14 Ma) to east (0.2 Ma) in an extensional ensialic back-arc setting as the west-dipping Adriatic plate delaminated and rolled back to the east (Serri *et al.*, 1993). In late Miocene time, the extensional processes affected the area of Elba Island (Bouillin *et al.*, 1993; Jolivet *et al.*, 1994), and several laccoliths, a major pluton, and an extensive dyke swarm were emplaced within stacked tectonic complexes.

2.2.2 Geological outlines of Elba Island

Elba Island was constructed from five tectonic complexes that were thrust onto each other by about 20 Ma (see Part III, Chapt. 1; Deino *et al.*, 1992). The lower three complexes have continental features, while the upper two are oceanic in character (Trevisan, 1950; Trevisan, 1953; Perrin, 1975; Keller and Pialli, 1990; Pertusati *et al.*, 1993). Complex IV consists of Jurassic oceanic lithosphere of the western Tethys Ocean (peridotite, gabbro, pillow basalt and ophiolite sedimentary breccia) and its upper Jurassic-middle

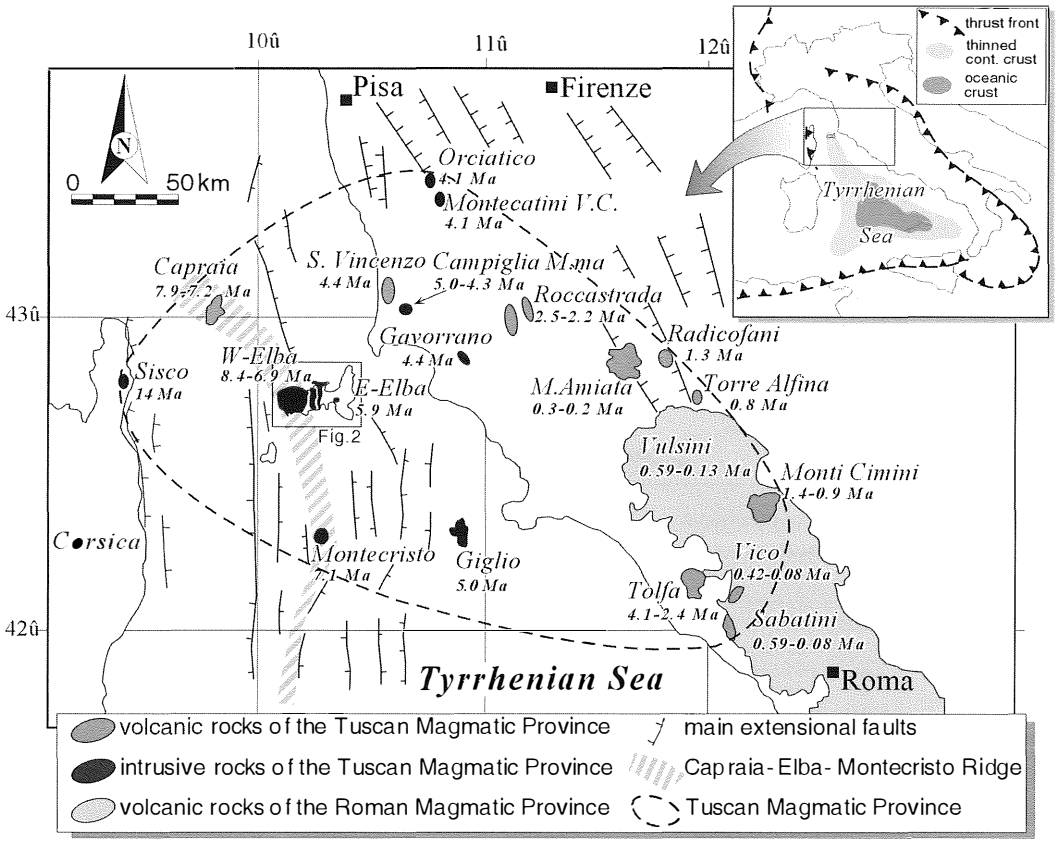

Fig. 1 – Location map for the Tuscan Magmatic Province. Also reported are the younger potassic-ultrapotassic volcanic rocks of the Roman Magmatic Province. Ages after the compilation of Serri *et al.* (2001).

Cretaceous sedimentary cover (chert, limestone, and argillite interbedded with siliceous limestone). Complex V consists of argillite, calcarenite and sandy marl of Palaeocene to middle Eocene age, overthrust by an upper Cretaceous flysch sequence (Bellincioni, 1958; Raggi *et al.*, 1965; Keller and Pialli, 1990).

Large-scale faults subdivided Elba Island into three geographic areas: western, central and eastern Elba (Fig. 2 and 3). Western Elba consists of the Monte Capanne monzogranitic pluton and its thermometamorphic carapace of Complex IV rocks that contain hypabyssal porphyry intrusions.

Western Elba is separated from central Elba by the Eastern Border fault that roughly parallels the east side of the Monte Capanne pluton, truncating its contact aureole and dipping moderately to steeply eastward (Fig. 2 and 3). For the most part, the fault is marked by a distinct plane separating a western footwall breccia of hornfelsed Complex IV rocks (ophiolitic material and deep marine cover rocks) plus fragments of the Monte Capanne pluton, from an eastern hanging wall breccia made of Complex V flysch and megacrystic San Martino porphyry.

Central Elba consists of Complex V flysch and enclosed porphyry intrusions, and is

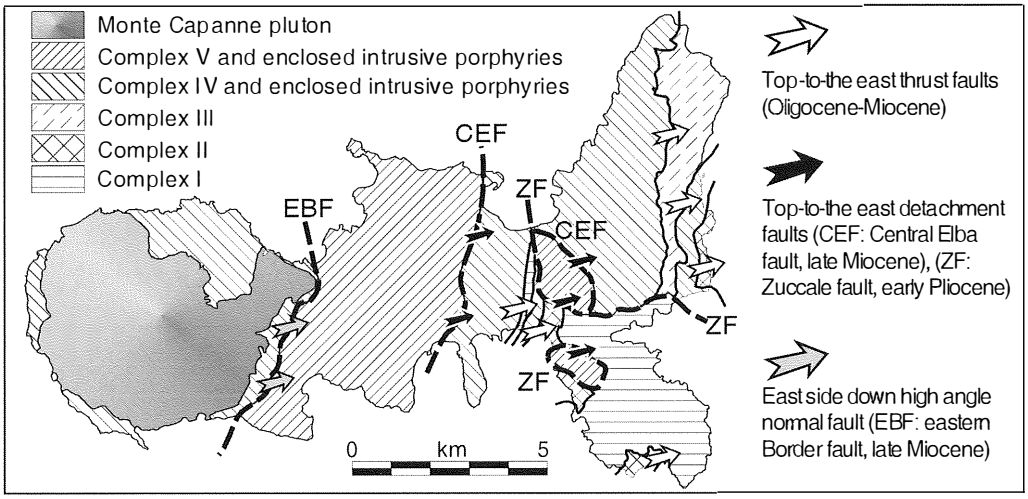

Fig. 2 – Tectonic sketch map of Elba Island.

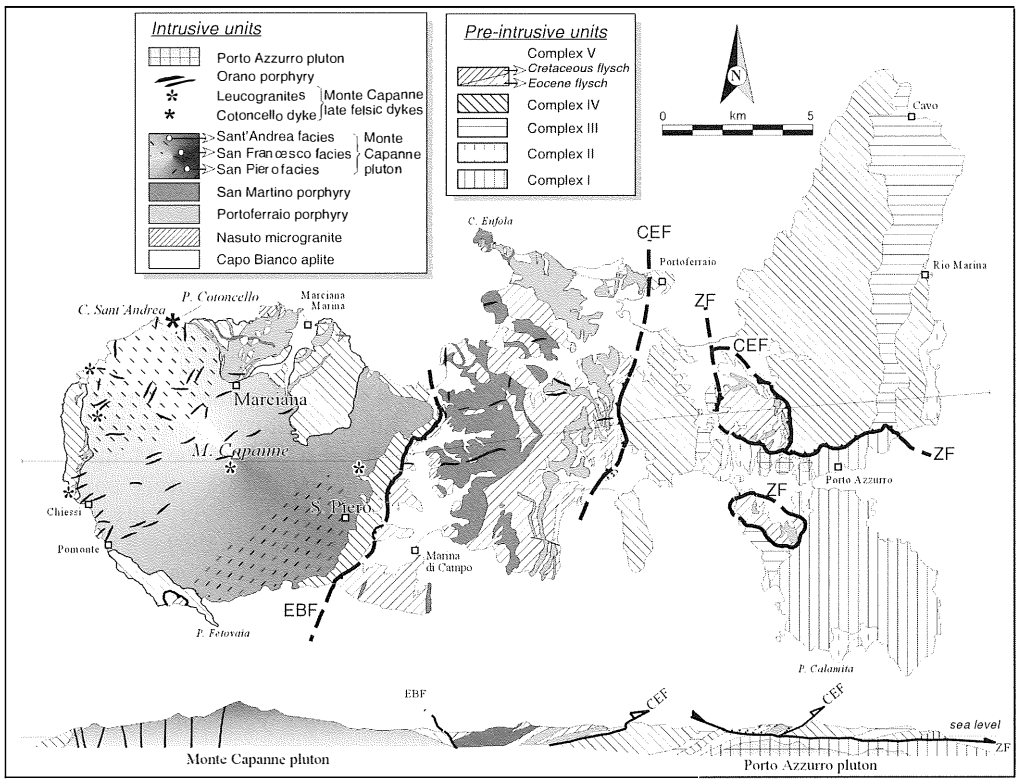

Fig. 3 – Geological map of Elba Island.

separated from eastern Elba by the low-angle Central Elba fault (Fig. 2 and 3) expressed as a tectonic mÈlange of rocks from Complexes IV and V (Trevisan, 1950; Bellincioni, 1958; Perrin *et al.*, 1975), including rocks whose equivalents crop out in western Elba. Thus, the rocks of central Elba were most likely displaced about 10 km eastward from their original position by way of movement on the Central Elba fault (Westerman *et al.*, submitted).

Eastern Elba consists of a stack of tectonic complexes. The upper portion of the stack, including part of the contact aureole of the upper Pliocene Porto Azzurro pluton, was displaced eastward by 5-6 km along the Zuccale fault (Keller and Pialli, 1990; Pertusati *et al.*, 1993) whose activity is geometrically and kinematically similar to that inferred for the Central Elba fault.

2.3 The intrusive units and sequence

Within Complex IV (western Elba) and Complex V (central Elba), distinction of the various intrusive units and their correlation between exposures is based on the consistent textural and mineralogical aspects of each unit (Table 1), and on consistent crosscutting relationships. Additional support comes from mineral chemistry and from major and trace element whole-rock data. All the different rock types are classified with the intrusive nomenclature after the Q'-ANOR diagram (Fig. 4; Streckeisen and Le Maitre, 1979). Indeed, despite the occurrence of high-temperature phases in some porphyritic dykes, all the studied units belong to a unique intermediate- to shallow-level intrusive complex.

Igneous products in eastern Elba are discussed here for thoroughness, but have not been the focus of detailed study by the authors.

2.3.1 Capo Bianco aplite

The Capo Bianco aplite is a white porphyritic rock with alkali feldspar granite compositions (Fig. 4). It occurs in western Elba within Complex IV as four adjacent, but isolated, caps on a ridge (Fig. 3), interpreted as an original sill dismembered by younger intrusions. The outcrops in central Elba make up a structurally higher tourmaline-rich laccolith layer (Westerman *et al.*, submitted). Whole rock-muscovite Rb-Sr isochrons (Ms phenocrysts >350 μm selected to avoid secondary sericite) yielded cooling ages of 7.95 ± 0.1 Ma and 7.91 ± 0.1 Ma for samples from western and central Elba, respectively (Dini *et al.*, 2002). A ^{40}Ar-^{39}Ar age older than 8.5 Ma for late magmatic muscovite from central Elba is reported by (Maineri *et al.*, 2003). In minor outcrops of Capo Bianco aplite which experienced eastward tectonic translation to eastern Elba (Pertusati *et al.*, 1993), the original rock is affected by hydrothermal recrystallisation of albite to sericite, a process dated at 6.7 ± 0.1 Ma (Maineri *et al.*, 2003). The isotopic ratios of the Capo Bianco aplite are, then, corrected to 8 Ma.

2.3.2 Nasuto Microgranite

The Nasuto microgranite, with a syenogranitic composition (Fig. 4), crops out over an area of 0.5 km^2 along the northern shore of western Elba (Fig. 3). It is entirely surrounded and intruded by the younger Portoferraio porphyry.

2.3.3 Portoferraio porphyry

The Portoferraio porphyry has dominantly monzogranitic, with minor syenogranitic, compositions (Fig. 4), with biotite having Fe# ranging from 0.45 to 0.50 (Fig. 5). These porphyries occur as major laccolith layers up to 700 m thick (Fig. 3), commonly interconnected, and as numerous dykes (Westerman *et al.*, submitted).

A Rb-Sr wr-Bt isochron points to an age of 8.4±0.1 Ma, but internal isotopic disequilibrium is suggested by the fact that initial $^{87}Sr/^{86}Sr$ ratios for plagioclase and K-feldspar deviate significantly from the isochron intercept (Dini, 1997). Thus, the interpretation

TABLE 1

Summary of petrographic and chronological features of the late Miocene intrusive units from Elba Island (modified after Dini et al., 2002).

Intrusive unit		Rock type	Texture	Paragenesis	Accessories	MME	Xenoliths	Age (Ma)
Monte Castello dyke		shoshonite	sub-aphyric	pheno: Cpx, Ol ghosts xeno: Pl, Kfs, Qtz gm: Cpx, Pl, San	Mag, Chr	no	no	5.83±0.14
Porto Azzurro pluton		monzogranite	Qtz±Pl phenocrysts medium-grained equigranular matrix	Pl, Qtz, Kfs, Bt	Zrc	no	no	5.9±0.2
Orano porphyry	granodioritic type	granodiorite to qtz monzodiorite	porphyritic (<20%) very fine-grained gm	pheno: Pl, Bt, rare Amph, Cps relics xeno: Kfs, Qtz	Ap, Zrc, Aln, Thr, Mag, Ilm, Per	common	rare (1-3cm)	6.83±0.06 6.87±0.30
	monzogranitic type	monzogranite	porphyritic (25-35%) fine-grained	gm: Pl, Mg-Bt, Qtz, Kfs				
Late felsic dykes associated with the Monte Capanne pluton	Leucogranite dykes	syenogranite	medium grain size locally anisotropic	Qtz, Kfs, Pl, Bt, Ms ± Crd or Grt	Ap, Zrc, Mnz, Tur	no	no	coeval with Monte Monte Capanne pluton
	Contoncello dyke	syenogranite	very low % megaKfs fine-grained matrix	Pl, Qtz, Kfs, Bt	Ap, Zrc, Mnz, Ilm	common (1-3 cm)	no	
	San Piero facies	monzogranite to granodiorite	very low % megaKfs fine-medium grained equigranular matrix	Pl, Qtz, Kfs, Bt	Ap, Zrc, Mon, Aln, Tur	low vol% (5 cm-1 m)	scattered (1-5 cm)	

TABLE 1 CONTINUED

Intrusive unit		Rock type	Texture	Paragenesis	Accessories	MME	Xenoliths	Age (Ma)
Monte Capanne pluton	Sant'Andrea facies	monzogranite	~20-30 vol% megaKfs medium-coarse grained	Pl, Qtz (up to 15 mm), Kfs (up to 15 cm), Bt (up to 5 mm)	Ap, Zrc, Mon, Aln, Ilm Tur	variable, up to 70 vol% (0.1-10m)	scattered (1-5 cm)	6.9 (see text for details)
	San Francesco facies	monzogranite	variable % megaKfs (5-9 cm) medium-gr. equigranular matrix	Pl, Qtz, Kfs, Bt	Ap, Zrc, Mon, Aln, Tur	variable vol% n 1/m2 (5 cm-5m)	scattered (1-5 cm)	
San Martino porphyry		monzogranite	porphyritic (40-50%) fine-grained gm miarolitic cavities	mega: San (3-15%; ~5 cm); pheno: Qtz, Pl, Bt; gm: Qtz, Kfs ±Pl	Ap, Zrc, Mon ± Aln±Tur	common 1/10 m2 (2 cm - 2 m)	common (1-10 cm)	7.2±0.1 7.44±0.08
Portoferraio porphyry		monzogranite (minor syenogr.)	porphyritic (25-50%) fine-grained gm	pheno: San, Qtz, Pl, Bt; gm: Qtz, Kfs ±Pl	Ap, Zrc, Aln, Mon, Thr	no	rare (1-3cm)	8.4±0.1
Nasuto microgranite		monzogranite	porphyritic (25-30%) microgranular gm	pheno: Qtz, Pl, Kfs, Bt; gm: Qtz, Kfs, Pl		no	no	
Capo Bianco aplite		alkali feldspar granite	porphyritic trachytoid gm	pheno: Qtz, Pl, Kfs, Ms; gm: Ab	Tur abundant in central Elba; Xen, Mon, Nb-Ta oxides	no	no	7.91±0.1 7.95±0.1 > 8.5

Abbreviations: Ab: albite; Aln; allanite; Ap: apatite; Bt: biotite; Crd: cordierite; Grt: garnet; Ilm: ilmenite; Mag: magnetite; Mon: monazite; Ms: muscovite; Per: perrierite; Pl: plagioclase; Qtz: quartz; San: sanidine; Thr: uraniferous thorite; Tur: tourmaline; Xen: xenotime; Zrc: zircon; mega: megacrysts (>2 cm); pheno: phenocrysts (< 2 cm); xeno: xenocrysts; gm: groundmass.

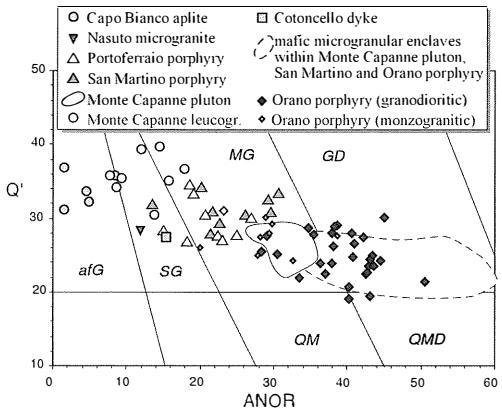

Fig. 4 – Q'-ANOR classification diagram (Streckeisen and Le Maitre, 1979). Abbreviations of rock names: afG, alkali feldspar granite; SG, syenogranite; MG, monzogranite; GD, granodiorite; QM, quartz monzonite; QMD, quartz monzodiorite. Modified after Dini *et al.* (2002).

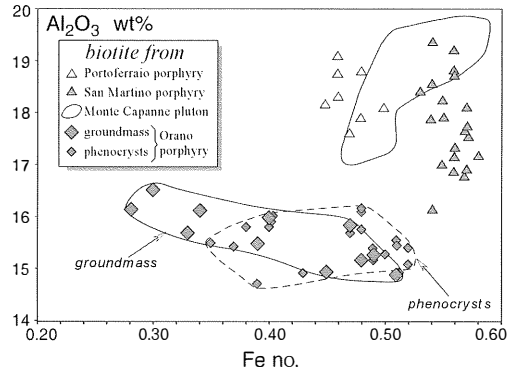

Fig. 5 – Al_2O_3 vs. Fe# (Fe/(Fe+Mg) atomic ratios) for biotites from the Elba intrusive units. Modified after Dini *et al.* (2002).

of the Rb-Sr age is constrained by the field evidence showing the Portoferraio porphyry as younger than the Capo Bianco aplite and older than the San Martino porphyry. For the purpose of this work, we chose to correct isotopic ratios for the Portoferraio porphyry to 8 Ma. Correction to 8.5 Ma would lead to deviations in $^{87}Sr/^{86}Sr$ of 2-3 times the analytical error, and to deviations in $^{143}Nd/^{144}Nd$ within the error.

2.3.4 San Martino porphyry

The San Martino porphyry has monzogranitic compositions (Fig. 4), and is characterised by prominent K-feldspar megacrysts and biotite with Fe# = 0.53 - 0.58 (Fig. 5), This unit occurs in western Elba as dykes cutting the Capo Bianco aplite and Portoferraio porphyry (Fig. 3), whereas in central Elba, it occurs as three main laccolith layers up to 400 m thick and as minor crosscutting dykes (Westerman *et al.*, submitted).

A Rb-Sr wr-Pl-Bt isochron indicates an age of 7.2 ± 0.1 Ma (Dini, 1997). However, significant Sr isotopic disequilibrium exists within K-feldspar, and between megacrysts and the whole rock. Nevertheless, this Rb-Sr date is quite close to a sanidine $^{40}Ar/^{39}Ar$ isochron age of 7.44 ± 0.08 Ma (Dini and Laurenzi, 1999). Initial isotopic ratios are then corrected to 7.4 Ma. Isotopic dates are in agreement with field observations and indicate that the San Martino porphyry was emplaced after a significant period of quiescence.

2.3.5 Monte Capanne pluton

The Monte Capanne monzogranitic pluton is the largest of those exposed in the Tuscan Magmatic Province (Marinelli, 1955; Marinelli, 1959; Poli *et al.*, 1989; Bussy, 1990; Poli, 1992). It is roughly circular in plan (about 10 km in diameter), and is bordered along two thirds of its perimeter by contact metamorphosed rocks mainly after Complex IV protoliths (Fig. 3).

The pluton shows minor variability of its petrographic features, but internal facies with diffuse transitions have been identified in the field (Fig. 3). They include as end members the «Sant'Andrea facies» and the «San Piero facies», separated by a wide zone of «San Francesco facies» having transitional characteristics. The two extreme facies are easily distinguished by their textures: the Sant'Andrea facies exhibits high percentages of coarse phenocrysts (Kfs, Qz, Bt) while the San

Piero facies appears mostly as a homogeneous, fine- to medium-grained rock almost devoid of early, coarse phenocrysts, while amphibole clots replacing former pyroxene are found. This petrographic subdivision of the pluton is supported by structural studies (Boccaletti and Papini, 1989) that identified a strong NNE-SSW preferred orientation of minerals in the south-eastern region (roughly corresponding to the San Piero facies), in contrast with the more irregular fabrics found in the northwestern part of the pluton. This pattern is also mimicked by those derived from AMS data (Bouillin *et al.*, 1993).

The whole intrusive mass is characterised by the widespread occurrence of mafic microgranular enclaves of varying amounts and sizes. These enclaves vary in composition from tonalite to monzogranite and consist principally of fine-grained plagioclase laths and biotite, with varying quantities of generally rounded and resorbed xenocrysts of quartz and K-feldspar. Plagioclase typically exhibits oscillatory zoning (An content up to 45%), and amphibole clots replacing former pyroxene are common. Two distinct types of megacrystic K-feldspar xenocrysts occur in these enclaves, one with poikilitic margins including matrix minerals, and the other with andesine-oligoclase borders. Mafic microgranular enclaves are characteristically less abundant in the south-eastern facies than in the main (normal).

Dates for emplacement of the Monte Capanne pluton are quite scattered (Juteau *et al.*, 1984; Ferrara and Tonarini, 1985), with Rb-Sr and U-Pb dates between 5.8 and 7.0 Ma. None the less, dates obtained for the late, post-plutonic Orano porphyry dykes (6.83 - 6.87 Ma, e.g. Section 3.g.) suggest that the most likely emplacement age for the Monte Capanne pluton is close to the highest literature values, i.e. 6.8 - 7.0 Ma (Dini *et al.*, 2002). Additionally, two samples from the San Piero facies display full Sr isotopic equilibrium and Rb-Sr wr-Pl-Kfs-Bt cooling ages of 6.88 ± 0.1 and 6.75 ± 0.07 (Innocenti *et al.*, 1992). Therefore, initial isotopic ratios of samples from the Monte Capanne pluton have been corrected to 6.9 Ma.

2.3.6 Late felsic products associated with the Monte Capanne pluton

The main pluton is cut by several felsic units, identified by their field characteristics as the Cotoncello dyke, the leucogranite dykes and the aplite-pegmatite veins and dykes. At Punta del Cotoncello (Fig. 3), the syenogranitic Cotoncello dyke exhibits a modest K-feldspar megacryst content and a distinctively finer-grained matrix than the Sant'Andrea facies of the main pluton which it cuts. This dyke strikes roughly parallel to the external contact of the pluton over a distance of more than 500 m, with a maximum thickness of about 100 m.

The leucogranite dykes also have syenogranitic compositions (Fig. 4), and they occur mainly close to the pluton's contact, within both the pluton and its thermometamorphic aureole. They commonly have thicknesses up to tens of meters. These dykes were emplaced late in the crystallisation sequence of the Monte Capanne pluton, and are locally cut by dykes of the Orano porphyry. We consider their emplacement age as indistinguishable from that of the Monte Capanne pluton. Aplite-pegmatite veins and dykes occur commonly as thin (0.1 to 2 m) and short (up to a few m) masses, in some places crosscutting the leucogranite dykes.

2.3.7 Orano porphyry

The Orano porphyry unit is an E-W-trending swarm of nearly 100 darkly coloured dykes that crosscut all the other intrusive units of the sequence (Dini *et al.*, 2002). They are restricted in western Elba to the northwestern portion of the Monte Capanne pluton and its contact aureole (approximately 6 dykes/km^2); in central Elba, the Orano dykes crop out only in the northern part of the area (Fig. 3). Dyke thicknesses range from less than a meter up to a maximum of 50 m, and contacts with host rock are sharp and planar, although commonly with abrupt changes in orientation. Both zoned and unzoned dykes are recognised, the former being generally thicker and internally differentiated with abrupt transitions between

inner and outer zones. Outer border zones are typically a few 10's of centimetres thick and are distinguished from the inner zones by (i) finer grained groundmass, (ii) lower content of K-feldspar and quartz xenocrysts, mafic microgranular enclaves and xenoliths, and (iii) higher ferromagnesian mineral concentrations. The inner portions of zoned dykes have monzogranitic compositions (Fig. 4), and their xenocrysts are petrographically very similar to minerals of the Monte Capanne pluton. The borders of zoned dykes are petrographically comparable to the unzoned dykes and have granodiorite to quartz-monzodiorite compositions (Fig. 4). These unzoned Orano dykes show evidence of early magma mingling including (i) three populations of plagioclase phenocrysts having strong differences in composition and texture, (ii) groundmass biotite attaining lower Fe# with respect to phenocrysts (Fig. 5), (iii) rounded and embayed quartz and Kfs xenocrysts, and (iv) coexisting quartz and olivine plus clinopyroxene phenocrysts (generally replaced by tremolite-actinolite, Cr-clinochlore and Mg-phyllosilicates).

The Orano porphyry is the youngest intrusive unit in both western and central Elba (Dini *et al.*, 2002). A western Elba sample, bearing compositionally homogeneous biotite, yielded a wr-Bt Rb-Sr internal isochron of 7.06 ± 0.07 Ma, but minor Sr isotopic disequilibrium exists between phenocrysts and the whole rock. However, such disequilibrium is rather restricted, and a wr-Pl-Kfs-Bt Rb-Sr internal isochron gave an age of 6.87 ± 0.28 Ma (MSWD = 16). This date matches the sanidine $^{40}Ar/^{39}Ar$ isochron age of 6.83 ± 0.06 Ma obtained for a central Elba Orano dyke (Dini and Laurenzi, 1999). Initial isotopic ratios were corrected to 6.85 Ma, accounting for a cooling age for Orano dykes that is essentially the same as that of the Monte Capanne pluton.

2.3.8 La Serra-Porto Azzurro pluton

Small outcrops of a monzogranite body are interpreted as evidence for the occurrence of a pluton in the Porto Azzurro area. The composition of samples (Conticelli *et al.*, 2001b) is similar to the most acidic portions of the Monte Capanne pluton, and the emplacement age is constrained at 5.9 Ma (Maineri *et al.*, 2003).

2.3.9 Monte Castello dyke

A grey-brownish porphyritic dyke is found in eastern Elba (Conticelli *et al.*, 2001b). The rock is quite altered, and the original phenocryst assemblage was constituted of plagioclase, clinopyroxene, olivine and scattered K-feldspar megacrysts of likely exotic origin. The dyke had an original shoshonite composition, and an emplacement age of 5.8 Ma (Conticelli *et al.*, 2001b). Its petrographic and geochemical feature resemble those of the Orano dykes, and also the close age relations to the Porto Azzurro pluton resemble those between the Orano dyke swarm and the Monte Capanne pluton. Thus, similar pluton-mafic dykes history occurred in western Elba at 6.9-6.8 Ma, an in eastern Elba 1 myr later.

2.3.10 Summary

The igneous sequence of western-central Elba started with construction of a laccolith complex, first by emplacement of the Capo Bianco aplite and Nasuto microgranite, followed in succession by the Portoferraio porphyry and, after a time lag of ca. 1 myr, the San Martino porphyry. The deepest layers of this complex were then intruded and/or deformed by the Monte Capanne pluton and its associated late leucocratic dykes and veins. Finally, the Orano dyke swarm was emplaced, cutting through the entire succession. Shortly thereafter, the upper part of the sequence, along with its host of Complex V flysch, was tectonically translated eastward so that the lower part is presently found in western Elba while the upper part is in central Elba (Rocchi *et al.*, 2002).

The emplacement of a pluton-mafic dyke association and tectonic translation of the upper part of the complex took place also in eastern Elba, 1 myr later.

2.4 Geochemistry and Petrogenesis

2.4.1 Geochemistry

Major elements. The intrusive units of the Elba igneous complex display limited intra-unit compositional variations, but significant inter-unit geochemical variability (Dini *et al.*, 2002; Table 2, Figs. 6, 7). All the intrusive units of the laccolith complex, which were emplaced before the Monte Capanne pluton, together with the pluton itself and its associated late felsic products, are made up of acidic rocks having SiO_2 in the range from 66.2 to 75.7 wt%. In contrast, the younger Orano porphyry is more mafic and shows lower SiO_2 contents between 62.8 and 66.9 wt %.

The Monte Capanne pluton shows restricted chemical variations (Figs. 6, 7). The whole pluton has monzogranite composition (SiO_2 between 66 and 70 wt%), and slightly peraluminous character (average ASI = 1.11 ± 0.05 1sd). Although three facies are recognised petrographically, they differ only slightly from each other chemically and thus are reported as a single field in Figures 4, 6 and 7. Due to the relative chemical homogeneity of the pluton and to its volumetric importance with respect to all the other intrusive units, descriptions of chemical data will be made in relation to the Monte Capanne pluton except where otherwise noted.

The intrusive units of the pre-pluton laccolith complex are more acidic than the pluton. Even though the entire intrusive assemblage shows MgO, FeO_{tot}, CaO and total alkalis vs. SiO_2 with general negative correlations (Figs. 6, 7), the SiO_2 vs. Al_2O_3 diagram discriminates between the intrusive units on the basis of both elemental abundances and elemental ratios (Fig. 7).

The Capo Bianco aplite, with the highest combined SiO_2 and Al_2O_3, defines a completely separate narrow field with the steepest Al_2O_3/SiO_2 slope (Fig. 7). These rocks also have extremely low TiO_2, FeO_{tot}, MgO and CaO, and a strong peraluminosity (average ASI = 1.42 ± 0.10, Table 2). The Nasuto microgranite, the Portoferraio porphyry and San Martino porphyry have overlapping major element characteristics, with combined SiO_2 and Al_2O_3 values higher than the Monte Capanne pluton and with a steeper Al_2O_3/SiO_2 slope (Fig. 7). The Nasuto microgranite is the most peraluminous of the three units (ASI = 1.29) and has slightly higher alkali content (Fig. 6). Major element chemistry of the monzogranitic Portoferraio porphyry (ASI = 1.18 ± 0.07) and San Martino porphyry (ASI = 1.22 ± 0.16, Table 2) overlap in every respect, although Portoferraio rocks are, on average, more alkaline and richer in SiO_2 and Al_2O_3 (Figs 5, 6) and have biotites with lower Fe# (Fig. 5).

The late-plutonic felsic products are chemically distinct from the Monte Capanne pluton and from each other (Figs 5, 6). The peraluminous Cotoncello dyke sample (ASI = 1.16) plots close to the silica-rich end of the Monte Capanne field and overlaps the compositional fields of the Portoferraio and San Martino porphyries. In contrast, the leucogranite dykes have the highest SiO_2 and lowest Al_2O_3 contents of the analysed rocks from the Elba magmatic complex, and their Al_2O_3/SiO_2 trend plots as an extension of the Monte Capanne pluton field.

Trace elements. The trace element distribution of the Monte Capanne pluton has low variability (Fig. 7) and the distribution of REE is homogeneous throughout the pluton (Dini *et al.*, 2002; Fig. 8). Again, the Capo Bianco aplite shows peculiar features. The Be and Cs contents of the Capo Bianco aplite are notably high (up to 67 and 131 ppm, respectively); Rb, Nb and Ta have the highest concentrations among the Elba igneous rocks, while Y ranges from the lowest to the highest values; Sr is low, and Zr, Ba and Th have the lowest values for Elba intrusives (Table 2; Fig. 6). The flat chondritic REE patterns (La_N/Yb_N = 1.3 - 2.2) with a very deep Eu trough (Eu/Eu* = 0.04 - 0.14) readily distinguish the Capo Bianco aplite from all the other units. Worth noting is the anomalously low Nd content, with Nd_N/Sm_N <1. The Nasuto microgranite has high Rb relative to rocks of

TABLE 2

Average major element chemical compositions for late Miocene intrusive units from Elba Island

unit	Capo Bianco aplite		Nasuto microgr.	Porto-ferraio porphyry		San Martino porphyry		Monte Capanne pluton		Monte Capanne leucogranites		Orano normal dyke swarm		Orano hybrid dyke swarm		Porto Azzurro pluton		Monte Castello dyke	
	average	*stdev*	PP-706	average	*stdev*	average	*stdev*	average	*stdev*	average	*stdev*	average	*stdev*	average	*stdev*	average	*stdev*	average	*stdev*
n. samples	6		1	10		10		23		9		28		8		4		2	
SiO_2	73.07	*0.66*	69.10	69.92	*1.38*	68.78	*1.41*	67.46	*0.83*	74.38	*1.17*	65.08	*1.49*	67.46	*1.17*	70.35	*0.22*	50.30	*0.71*
TiO_2	0.02	*0.01*	0.36	0.29	*0.04*	0.36	*0.03*	0.56	*0.05*	0.17	*0.07*	0.60	*0.05*	0.48	*0.05*	0.44	*0.04*	0.79	*0.01*
Al_2O_3	16.59	*0.57*	16.45	15.82	*0.62*	16.28	*0.47*	15.89	*0.27*	14.09	*0.43*	15.76	*0.43*	15.81	*0.35*	15.40	*0.41*	15.15	*0.35*
Fe_2O_3	0.23	*0.11*	0.40	0.50	*0.18*	0.52	*0.20*	0.79	*0.20*	0.53	*0.21*	1.08	*0.42*	0.90	*0.34*	0.95	*0.51*	2.28	*0.08*
FeO	0.23	*0.08*	1.54	1.24	*0.23*	1.56	*0.30*	2.35	*0.25*	0.49	*0.29*	2.74	*0.32*	2.15	*0.51*	1.67	*0.55*	4.57	*0.41*
MnO	0.05	*0.03*	0.04	0.03	*0.01*	0.04	*0.01*	0.06	*0.01*	0.03	*0.01*	0.06	*0.01*	0.05	*0.01*	0.04	*0.01*	0.13	*0.01*
MgO	0.09	*0.07*	0.99	0.85	*0.17*	0.94	*0.16*	1.41	*0.29*	0.36	*0.19*	2.62	*0.76*	1.61	*0.29*	0.92	*0.15*	6.23	*0.14*
CaO	0.22	*0.14*	0.83	1.57	*0.29*	2.11	*1.09*	2.62	*0.24*	0.94	*0.26*	3.15	*0.62*	2.22	*0.36*	1.76	*0.28*	6.63	*0.45*
Na_2O	4.24	*0.35*	3.82	3.60	*0.28*	3.38	*0.30*	3.48	*0.34*	3.20	*0.36*	3.22	*0.22*	3.55	*0.49*	3.24	*0.14*	2.24	*0.53*
K_2O	4.06	*0.10*	4.71	4.50	*0.26*	4.23	*0.42*	4.08	*0.23*	5.07	*0.73*	3.65	*0.30*	4.04	*0.66*	4.21	*0.10*	3.41	*0.56*
P_2O_5	0.02	*0.01*	0.06	0.10	*0.02*	0.14	*0.02*	0.20	*0.03*	0.06	*0.03*	0.19	*0.04*	0.19	*0.03*	0.17	*0.04*	0.15	*0.01*
LOI	1.26	*0.08*	1.69	1.60	*0.80*	1.99	*0.95*	1.08	*0.26*	0.68	*0.22*	1.75	*1.12*	1.54	*0.51*	0.85	*0.15*	8.14	*0.54*
ASI	1.42	*0.10*	1.29	1.18	*0.07*	1.22	*0.16*	1.10	*0.04*	1.15	*0.05*	1.09	*0.09*	1.15	*0.08*	1.22	*0.10*	8.14	*0.54*

Abbreviation: ASI: Alumina Saturation Index, corrected for the apatite content. Orano normal: thin dikes and border facies of thick dikes. Orano hybrid: inner facies of thick dikes. Porto Azzurro: data from Conticelli *et al.*(2001) and unpublished data from the authors. monte Castello dyke: data from Conticelli *et al.*(2001).

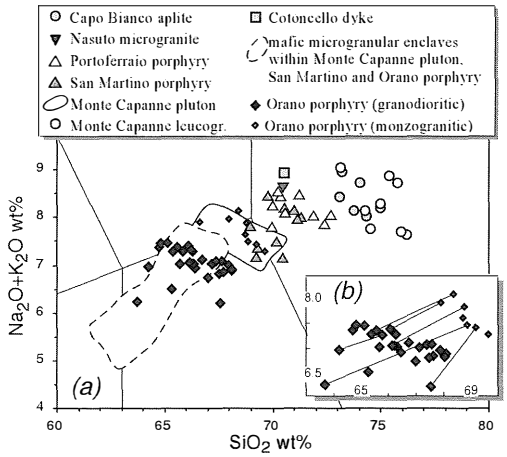

Fig. 6 – (a) Total alkali vs. silica (TAS) classification diagram (Le Bas *et al.*, 1986). (b) TAS enlargement for Orano dykes; tie-lines connect cores (larger symbol) and rims (smaller symbol) of individual dykes. Modified after Dini *et al.* (2002).

the Portoferraio and San Martino porphyries (Fig. 6), but shows an overall REE distribution similar to these units, albeit with a deeper Eu anomaly (Eu/Eu* = 0.27). The Portoferraio porphyry has uniform LREE distribution (La_N/Sm_N = 3.5 - 4.4), whereas the HREE fractionation is quite variable as shown by Gd_N/Yb_N = 2.1 - 3.9) and high and low Y contents (Fig. 6) which also correlate negatively with the Eu/Eu* ratios. The San Martino porphyry has constant REE distribution (La_N/Yb_N = 17.4 - 17.8 and Eu/Eu* = 0.51 - 0.52) with a pattern that is indistinguishable from that of the Monte Capanne pluton. Among the late felsic facies associated with the Monte Capanne pluton, the Cotoncello dyke has a HREE pattern (Gd_N/Yb_N = 3.7) more fractionated than the Monte Capanne rocks and similar to the low Y-HREE samples of the Portoferraio porphyry (Fig. 7). On the other hand, the leucogranite dykes show considerable overlap with the Capo Bianco aplite for many geochemical parameters, with REE fractionation intermediate between that of Monte Capanne pluton and the Capo Bianco aplite.

The post-plutonic Orano dyke swarm includes two compositional groups, monzogranitic samples from the core of thick zoned dykes, and granodioritic samples from borders of those dykes and from unzoned dykes (Table 1; Fig. 6). Compositions of the monzogranitic samples are intermediate between the Monte Capanne pluton and the granodioritic Orano group, and these xenocryst-rich rocks are interpreted as mixtures of Orano melt and solids from the Monte Capanne crystal mush, formed during emplacement of the dykes. The Orano porphyry has the lowest SiO_2 content of the Elba intrusive units, with values similar to those of mafic microgranular enclaves hosted in the Monte Capanne pluton, the San Martino porphyry, and the Orano dykes themselves. MgO (Fig. 6), as well as FeO_{tot} and TiO_2, shows strong variation over a rather restricted range of SiO_2 (62 - 68 wt%). The Orano porphyry has very distinctive overall trace element distribution. Some Orano porphyry samples display extreme enrichment in Sr, Ba, and LREE, which is oddly coupled with the highest Ni and Cr contents (Table 2; Fig. 6).

Also, REE fractionation reaches extreme values (La_N/Yb_N up to 59), coupled with moderate Eu anomalies (Eu/Eu* = 0.53 - 0.72). Despite the high variability of major element chemistry of the mafic microgranular enclaves (Figs. 6, 7), the analysed Orano enclave has REE distribution identical to samples from the Monte Capanne pluton, and is very similar to that of a San Martino enclave (Fig. 8).

Sr-Nd isotope composition. The Elba igneous products display wide variation in Sr isotopic ratios and bimodal distribution for Nd isotopic ratios (Dini *et al.*, 2002). The Capo Bianco aplites, Nasuto microgranite, Portoferraio porphyry and Cotoncello dyke make up a group with low $\varepsilon_{Nd}(t)$ values between -9.5 and -10.0 and strongly variable Sr isotopic ratios (0.7115 - 0.7228). The Monte Capanne pluton and its leucogranite dykes, along with the San Martino porphyry and all the mafic microgranular enclaves in the complex, make up a second group having

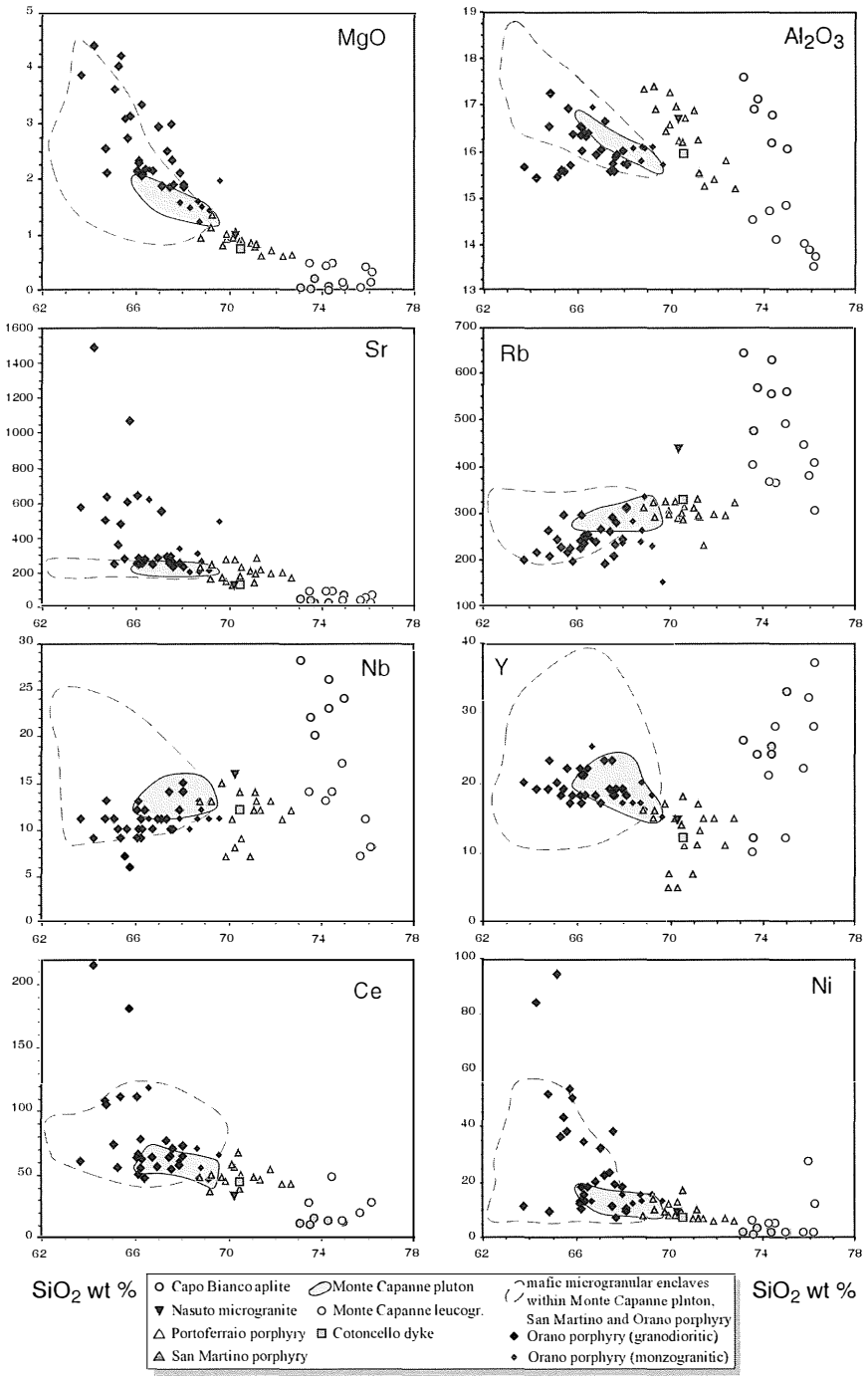

Fig. 7 – Variation diagrams for western-central Elba intrusive units, after Dini *et al.* (2002).

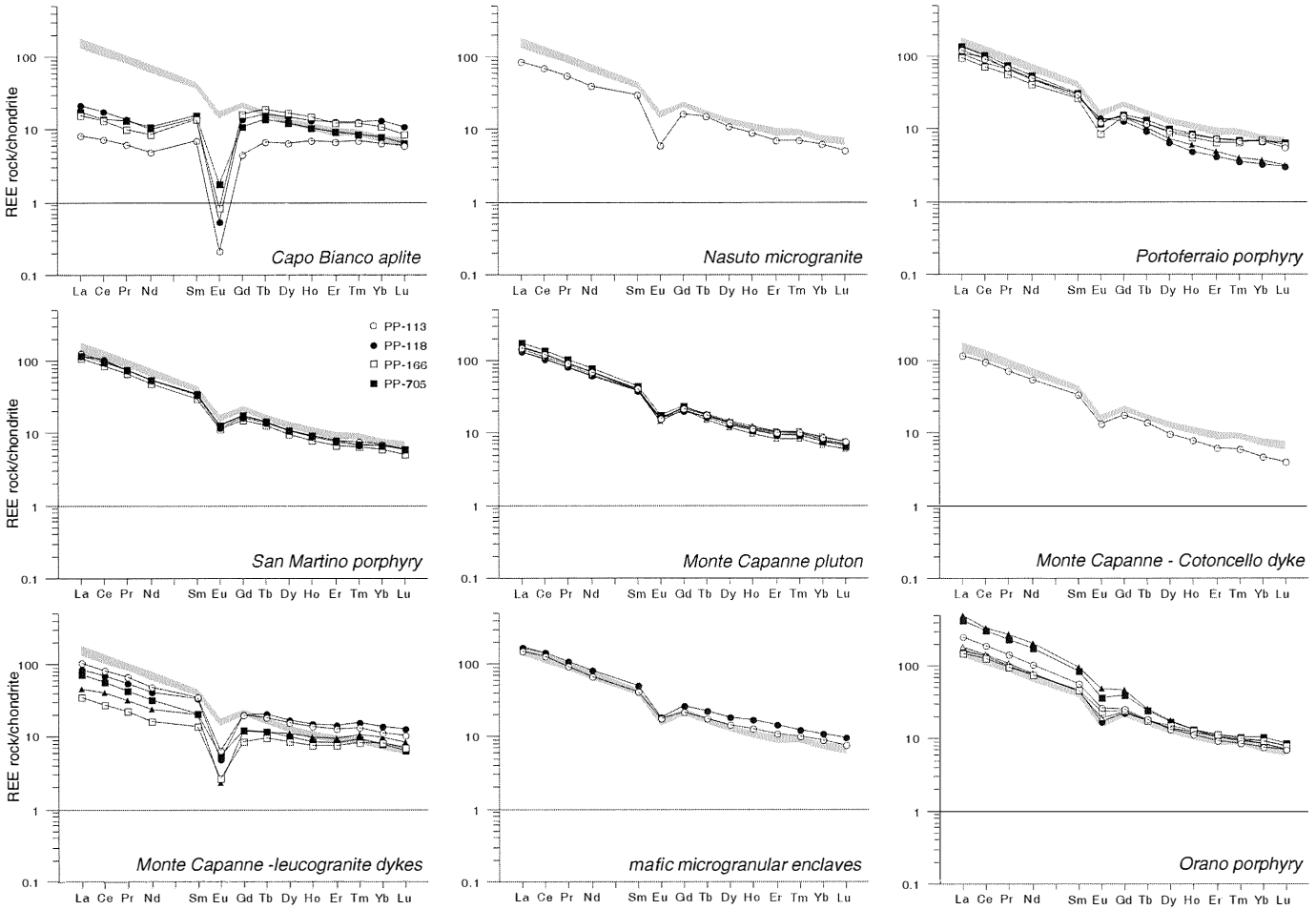

Fig. 8 – Chondrite-normalised REE patterns (McDonough and Sun, 1995) for Elba intrusives. The shaded field represents the REE compositional field for the Monte Capanne pluton. After Dini *et al.* (2002).

relatively high $\varepsilon_{Nd}(t)$ values between -8.1 and -8.9, and $^{87}Sr/^{86}Sr$ varying in the range 0.7131 - 0.7162. Samples of Orano porphyry constitute a third group that displays significant variation of $\varepsilon_{Nd}(t)$ between –7.0 and –10.1, while initial Sr isotopic ratios have a relatively restricted variation (0.7114 - 0.7138). The Orano porphyry has the lowest Sr and highest Nd isotopic ratios within the whole Elba intrusive complex. Isotopic ratios of mafic microgranular enclaves in the San Martino and Orano rocks are uniform and independent of the host. Enclaves from the San Martino porphyry have lower Sr and higher Nd isotopic ratios with respect to their host while enclaves from the Orano porphyry have higher Sr and lower Nd isotopic ratios than their host. In contrast, most of the analysed enclaves overlap those of the Monte Capanne host pluton. Interestingly, some mafic enclaves display unusual low $\varepsilon_{Nd}(t)$ [-9.84<$\varepsilon_{Nd}(t)$<-11.20] extending towards the field of the Tuscan lamproites (Gagnevin, pers. comm.). One cumulitic amphibole-bearing micro-gabbroic enclave sampled near San Piero displays the lowest $\varepsilon_{Nd}(t)$ (4.82) and initial Sr isotopic ratio (0.70928) recorded in the Monte Capanne pluton (Gagnevin, pers. comm.).

2.4.2 Petrogenesis

The intrusive and chronological relationships of the Elba igneous complex, coupled with the overall geochemical features and the strongly variable isotopic ratios, allow us to speculate about the origin of the different intrusive units from a number of different sources (Dini *et al.*, 2002). We recognise the Elba complex to include three isotopically distinct groups of rocks, as shown in Figure 9. Group 1 consists of the oldest units of the complex, i.e. the ca. 8 Ma intrusions of the Capo Bianco aplite, Nasuto microgranite and Portoferraio porphyry, along with the late-plutonic Cotoncello dyke, and is characterised by relatively low $\varepsilon_{Nd}(t)$ values. Group 2 is isotopically homogeneous, and consists of the San Martino porphyry, the Monte Capanne pluton, the leucogranite dykes, and all the mafic microgranular enclaves. These units were emplaced at ca. 7 Ma, and represent the bulk of the complex with a volume on the order of about 170 km^3. Group 3 rocks, namely the Orano dykes, constitute the youngest units of the complex and are characterised by strongly variable isotopic compositions, including the lowest Sr and highest Nd isotope ratios of the complex.

Group 1 - Crustal messengers. All the older (ca. 8 Ma) pre-plutonic intrusive units, and the younger, late-plutonic Cotoncello dyke, have compositional features matching those of both natural and experimental melts derived from metasedimentary crustal sources. These features are mainly represented by strong peraluminosity and high SiO_2 content, coupled with low concentrations of ferromagnesian elements (Patiño Douce, 1999). In the Capo Bianco aplite, significant internal geochemical variations exist that can be explained by mineral

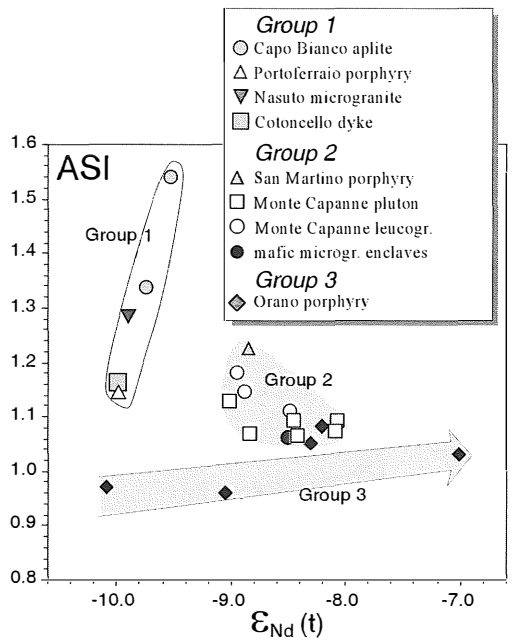

Fig. 9 – ASI (Alumina Saturation Index) vs. $\varepsilon_{Nd}(t)$ showing isotopically distinct groups of rocks from the Elba igneous complex. Modified after Dini *et al.* (2002).

fractionation. The major element compositions of the samples with extremely high Rb/Sr ratios can be modelled by removing less than 10 wt% of a plagioclase-dominated assemblage from the highest-Sr Capo Bianco sample. In the same way, the Rb/Sr vs. Sr and Ba trends are accounted for by removing about 20 wt% of the above assemblage (Fig. 10). On the other hand, the rocks with the lowest Rb/Sr ratio could have been produced by two alternative processes, either crystal fractionation from a less evolved parent magma, or direct melting of a crustal source. For the first alternative, extreme fractionation of K-feldspar, plagioclase, quartz and biotite would explain the major element compositions and the strongly negative Eu anomaly of these samples. Furthermore, removal of accessory minerals like monazite would be able to both flatten a typical granite-like REE pattern (see Monte Capanne REE pattern of Figure 7) and produce the unusually low Nd content relative to Pr and Sm. This is not, however, a physically viable process, unless accessories are hosted in biotite (Bea, 1996), a phase typically absent in the Capo Bianco aplite. Additionally, examination of SiO_2 vs. Al_2O_3 for the Elba intrusives (Fig. 6) shows that the Capo Bianco aplites define an isolated high silica - high aluminium field. Given the high aluminium content of feldspars, it is clear that the Capo Bianco aplites did not form by feldspar-dominated fractionation since any required parent magma would be unrealistically aluminous.

The second alternative, with direct melting of a crustal source, is a viable process. Indeed,

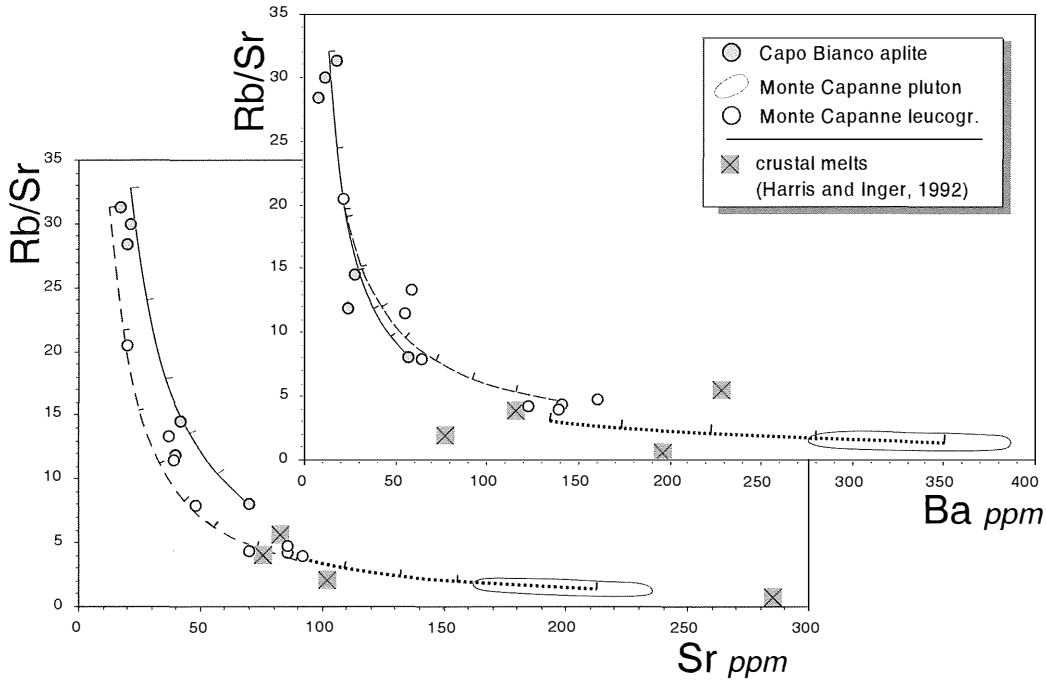

Fig. 10 – Rb/Sr vs. Ba and Sr diagrams to compare major and trace element compositions of possible crust-derived melts from Elba to calculated compositions (Harris and Inger, 1992). Fractional crystallisation lines for internal variations of Capo Bianco aplite and Monte Capanne microleucogranites are solid and dashed, respectively. Dotted lines shows fractional crystallisation of the average Monte Capanne pluton composition. Removed fractions are as discussed in the text; ticks are at 5% intervals. Modified after Dini *et al.* (2002).

both major and trace element compositions of those rocks having the lowest Rb/Sr ratio, Al_2O_3 content, and Na_2O/K_2O value (ca. 1), are comparable with compositions obtained for experimental melts from muscovite dehydration melting of pelitic sources at 0.8 GPa and 800°C (Patiño Douce and Harris, 1998). Moreover, muscovite dehydration melting can account for the deep negative Eu anomaly in a flat REE pattern with low LREE content. In fact, monazite, apatite and zircon are commonly armoured by biotite and, therefore, do not supply trace elements to the liquid, thus producing a Zr-P-LREE-poor melt (Nabelek and Glascock, 1995). Such a melt would have a negative Nd anomaly linked to the high partition coefficient of Nd in the restitic monazite, relative to its neighbours Ce-Pr and Sm (Yurimoto *et al.*, 1990). In summary, samples of the Capo Bianco aplite are interpreted as a direct product of muscovite dehydration melting of a metapelitic source. The Nasuto microgranite and Portoferraio porphyry also belong to the 8 Ma emplacement stage, and are, like the Capo Bianco aplite, strongly peraluminous. Such a strong «crustal» imprint suggests a direct derivation by crustal melting, and the significant content of ferromagnesian elements agrees with a process that involved biotite dehydration melting. Furthermore, the CaO enrichment in these rock, relative to ferromagnesian components, is consistent with derivation from a biotite-plagioclase-rich source such as metagreywacke, rather than a simple biotite-rich metapelite (Patiño Douce, 1999). The involvement of biotite together with its accessory minerals (e.g. monazite) can explain the more typical, «crustal» REE pattern of these units. Finally, the Cotoncello dyke is also definitely peraluminous and, as in the case of the Nasuto microgranite and Portoferraio porphyry, its distribution of major elements and REE pattern are consistent with derivation from a biotite-plagioclase-rich source. Furthermore, its high Sr isotopic composition points to a crustal origin and rules out derivation as a fractionation product of the Monte Capanne pluton.

Group 2 – Hybrids. The Monte Capanne pluton is an acidic, voluminous body with homogeneous geochemical features. Its low silica content, along with a ubiquitous presence of abundant mafic microgranular enclaves with isotopic ratios equal those of the pluton, amphibole clots after pyroxene, and plagioclase with calcic cores, all point to the involvement of more than one magma in the genesis of this pluton (Poli, 1992). The youngest pre-plutonic unit, the San Martino porphyry, displays geochemical and petrographic features similar to the Monte Capanne pluton, although the former is slightly more peraluminous and richer in SiO_2. Tonalitic mafic microgranular enclaves are common in this porphyry and the Sr-Nd isotopic composition of one of them is indistinguishable from that of the Monte Capanne pluton. This indicates that hybrid melts were available and mingled with peraluminous melts during emplacement of the San Martino magmas. The late leucogranite dykes of the Monte Capanne pluton show significant intra-unit geochemical variations (Figs. 6, 7, 8) that can be explained by invoking a process of mineral fractionation (e.g. Poli, 1992). Major element compositions of the samples with extremely high Rb/Sr ratios can be satisfactorily modelled by removing from the least acidic, highest- Sr samples, 13 wt% of a solid assemblage made up of plagioclase (80%; An_{16}), biotite (13%) and K-feldspar (7%). The Rb/Sr vs. Sr and Ba trends are also accounted for by removing up to 25 wt% of such an assemblage (Fig. 10). On the other hand, major element compositions of the least evolved leucogranites can be satisfactorily modelled by removal of a biotite-andesine assemblage from the average composition of Monte Capanne pluton equal to 30 - 35 wt% of that parent. The lack of K-feldspar in this fractionating assemblage makes the San Piero facies the most likely parent for the leucogranite melts since it was only in that facies that K-feldspar entered the liquidus assemblage late. Thus, we envisage the possibility that only low amounts of leucogranite melt were effectively separated

from the residue, and the bulk composition of the San Piero facies was not strongly modified. In conclusion, the leucogranites are interpreted as a series of fractionation products from a magma having characteristics similar to those of the San Piero facies of the Monte Capanne pluton, a hypothesis further supported by the overlapping Sr and Nd isotopic compositions of the Monte Capanne pluton and the leucogranite dykes.

Group 3 - Mantle messengers. The Orano dyke swarm consists of two petrographic types. The monzogranitic type is rich in xenocrysts captured from an acid crystal mush that matches well with the Monte Capanne pluton, so this group is not, therefore, a suitable source of information about original magmas. The granodioritic to quartz monzodioritic type, with only minor xenocrysts, still displays evidence for melt hybridism. However, these melts did contain phlogopite, as well as olivine and/or clinopyroxene, as a part of their liquidus assemblage. Additionally, these rocks have high Ni and Cr content coupled, in some samples, with extreme enrichment in Sr, Ba and LREE, and strong REE fractionation. Two samples from the Orano porphyry have been compared with mantle-derived magmas from the Tuscan Magmatic Province, i.e. the K-rich andesites from Capraia Island (e.g. Poli, 1992) and lamproites from mainland Tuscany (Fig. 11). These products all have similar overall distributions of incompatible trace elements, with highly fractionated NMORB normalised patterns, very high contents of the most incompatible elements, and high LILE/HFSE ratios. However, the Orano dykes most closely resemble the Capraia K-andesites with which they share overlapping Th/Ta values (Fig. 11). In addition, they lack the negative Sr anomaly which characterises the lamproites.

Regarding the isotopic data, $^{87}Sr/^{86}Sr(t)$ and $^{143}Nd/^{144}Nd(t)$ values of the Orano porphyry constitute the limits found in Elba intrusive rocks, i.e. 0.71145 and 0.51227, respectively, with the exception of the San Piero gabbroic enclave. These values are quite extreme for mantle-derived magmas; however, they are

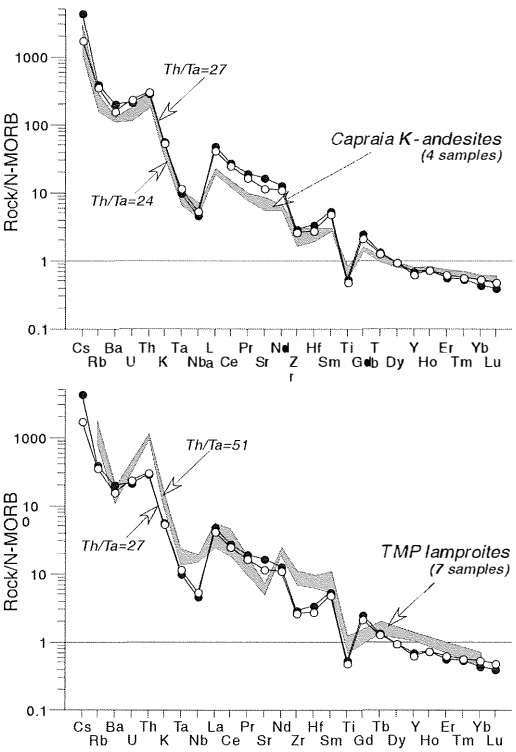

Fig. 11 – N-MORB normalised spidergrams (Sun and McDonough, 1989) of the most incompatible element-enriched Orano dyke (2 samples), compared with K-rich andesites from Capraia Island (D'Orazio, pers. comm.) and lamproites from the Tuscan Magmatic Province (Conticelli *et al.*, 1992). Modified after Dini *et al.* (2002).

coupled with very high Sr and Nd contents (1461 and 94 ppm respectively). Because crustal materials generally have much lower Sr and Nd contents, we conclude that these Orano isotopic ratios are very close to the original values of mantle-derived magma. Therefore, the anomalous isotopic ratios and trace element distribution are seen as evidence for an origin of Orano melts from a strongly modified mantle source, as is generally envisaged for the Tuscan Magmatic Province (Serri *et al.*, 1993; Peccerillo, 1999).

Sr and Nd isotope constraints on petrogenesis. The isotopic compositions of the crust-derived Group 1 units are significant in

understanding the nature of the crust involved as sources for the Elba magmas. These units have equivalent low $\varepsilon_{Nd}(t)$ values, coupled with strongly variable Sr isotope ratios (Fig. 12). Two main processes can be invoked to explain these isotopic features, namely melting of independent crustal sources with different $^{87}Sr/^{86}Sr$ ratios and uniform $\varepsilon_{Nd}(t)$ values, or melting of a Sr-Nd isotopically homogeneous crustal source under conditions able to differentiate the Sr isotopic ratios of the melt. The latter process can occur in the case of incongruent fluid-absent melting. Muscovite and/or biotite dehydration melting also involves K-feldspar and plagioclase, which have Rb/Sr ratios substantially lower than those of micas. The lack of a fluid phase can yield melts with a $^{87}Sr/^{86}Sr$ ratio either higher or lower than that of the source (Inger and Harris, 1993; Harris and Ayres, 1998), depending on the modal proportions of the phases entering the melt (mainly K-feldspar, plagioclase and mica) and on their Sr concentrations.

The modelling of Barbero *et al.* (1995) shows that when plagioclase makes up >30 modal% of the phases entering the melt, the melt has a $^{87}Sr/^{86}Sr$ ratio lower than that of the protolith, with a difference up to 0.004. This type of process could be invoked to explain the differences in Sr isotopic ratios between the Capo Bianco, Nasuto and Portoferraio units (<0.003), but it is not able to explain the large difference in $^{87}Sr/^{86}Sr$ ratio (0.011) occurring between the Capo Bianco and Cotoncello units.

On the basis of the above discussion, it is possible to conclude that the crustal sources activated at around 8 Ma and 7 Ma were different, at least isotopically (Dini *et al.*,

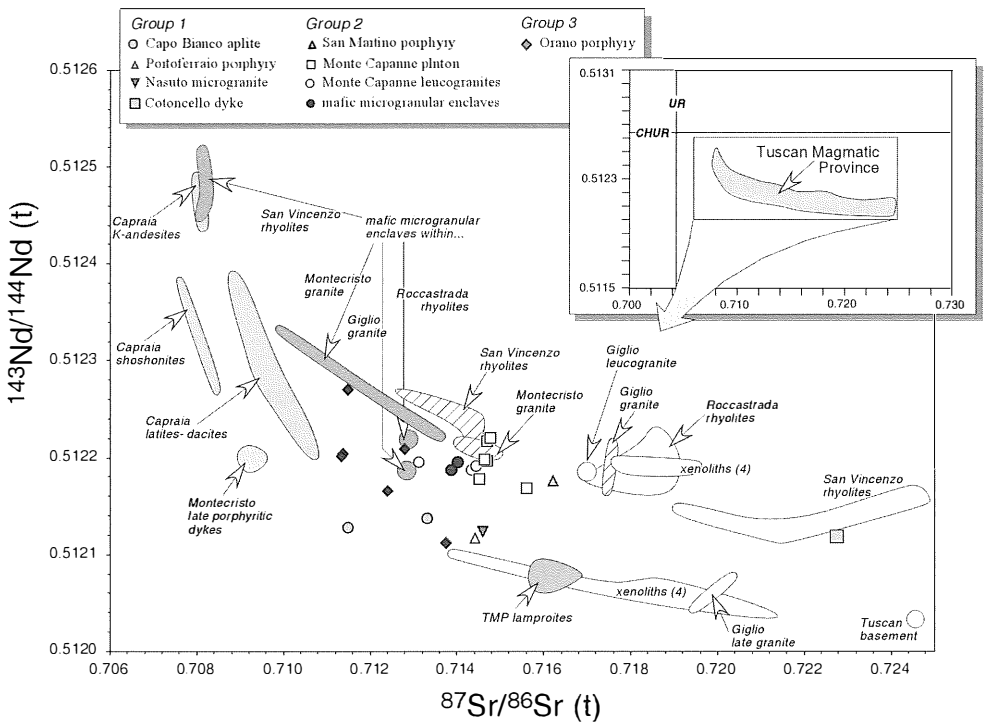

Fig. 12 – Initial $^{143}Nd/^{144}Nd$ vs. $^{87}Sr/^{86}Sr$ plot for studied samples and Tuscan Magmatic Province samples from the literature. Source of data: (Juteau *et al.*, 1984; 1986; Ferrara *et al.*, 1989; Pinarelli *et al.*, 1989; Westerman *et al.*, 1993; Innocenti and Tonarini (unpublished data). After Dini *et al.* (2002).

2002). A unique crustal source (Tuscan Crust-C1) could have been activated in the initial phases of melting to produce the Capo Bianco, Nasuto and Portoferraio magmas. In contrast, the source for the Cotoncello dyke represents a separate component (Tuscan Crust-C2) that is isotopically comparable with the crust-derived San Vincenzo rhyolites of the Tuscan Magmatic Province (Feldstein *et al.*, 1994; Ferrara *et al.*, 1989; Pinarelli *et al.*, 1989). Most of the Elba igneous rocks belong to the isotopically homogeneous Group 2, thought to be primarily generated by a hybridisation process. This hybrid system had to be large and homogeneous in order to sustain production of such significant amounts of compositionally constant magma. The general petrogenetic relationships of the materials involved in this process are illustrated in the $^{143}Nd/^{144}Nd$ vs. $^{87}Sr/^{86}Sr$ diagram of Figure 12, where the Elba data are plotted together with isotope variation fields of other Tuscan Magmatic Province rocks. Overall, the available data define two curvilinear trends pointing on the right toward two distinct crustal end-members with high Sr- and low Nd-isotope ratios, and, on the left, toward a mantle component with relatively low Sr and high Nd isotope ratios. The upper trend corresponds well with the mixing trend described for the San Vincenzo volcanics that relates mafic microgranular enclaves and their cordierite-bearing rhyolite host, considered as a nearly pure crustal melt (Ferrara *et al.*, 1989). The lower trend points to a crustal component with a lower Nd isotopic ratio, comparable with that observed in some Tuscan basement rocks (outcrops, cores and xenoliths; Fig. 12). Therefore, the occurrence of the two trends suggests that more than one crustal component has been involved in Tuscan Magmatic Province magmatism. Regarding the mantle-derived components involved in the mixing, K-rich andesites and basalts from Capraia (Tonarini, unpubl. data), and mafic microgranular enclaves from the San Vincenzo rhyolites seems to be the most likely candidates. The involvement of a mantle-derived magma similar to San Vincenzo mafic enclaves is also attested by the isotopic composition of the micro-gabbroic enclave from San Piero.

Additional insight into the evolution of the hybridised rocks of the Monte Capanne pluton and San Martino porphyries comes from examination of a $^{87}Sr/^{86}Sr$ vs. 1000/Sr diagram (Fig. 13a), in which most samples cluster at Sr ca. 200 ppm and $^{87}Sr/^{86}Sr$ ca. 0.7145. These values can, therefore, be regarded as the most likely to have developed during the hybridisation process as suggested by Poli (1992). This cluster of hybrid compositions can be obtained by a mixing process involving the Cotoncello dyke magma and Capraia K-andesites (close in space and time to the Elba igneous activity) whose source is here called Tuscan Mantle-M1. Moreover, the Capraia-Cotoncello mixing trend and its end-members are very similar to those inferred to explain San Vincenzo magmatism, where hybridism is well constrained (Ferrara *et al.*, 1989).

Examination of the plot of $^{143}Nd/^{144}Nd$ vs. 1000/Nd (Fig. 13b) confirms the above interpretation and suggests further insights concerning the origin of isotopic variations internal to the Orano porphyry whose samples plot well off the Capraia-Cotoncello mixing trend. The analysed samples of Orano dykes are distributed along a main linear trend with a few samples shifted horizontally into the field of hybrid magmas (Capraia-Cotoncello mixing trend). The steep trend starts from the LILE-richest sample previously identified as isotopically similar to the mantle end member for Orano magmas (from Tuscan Mantle-M2), and points to a felsic end member with a very low Nd isotopic ratio, even lower than the Group 1 end members, thus identifiable as coming from a different crustal source (Tuscan Crust-C3). A possible representative of this melt can be found in the late crustal leucogranite of Giglio Island (Le Scole intrusion; Westerman *et al.*, 1993). The horizontally shifted (Nd depleted) samples are interpreted as originating from a solid-liquid mixture with Monte Capanne magmas. Thus, Orano magma does not represent the mantle

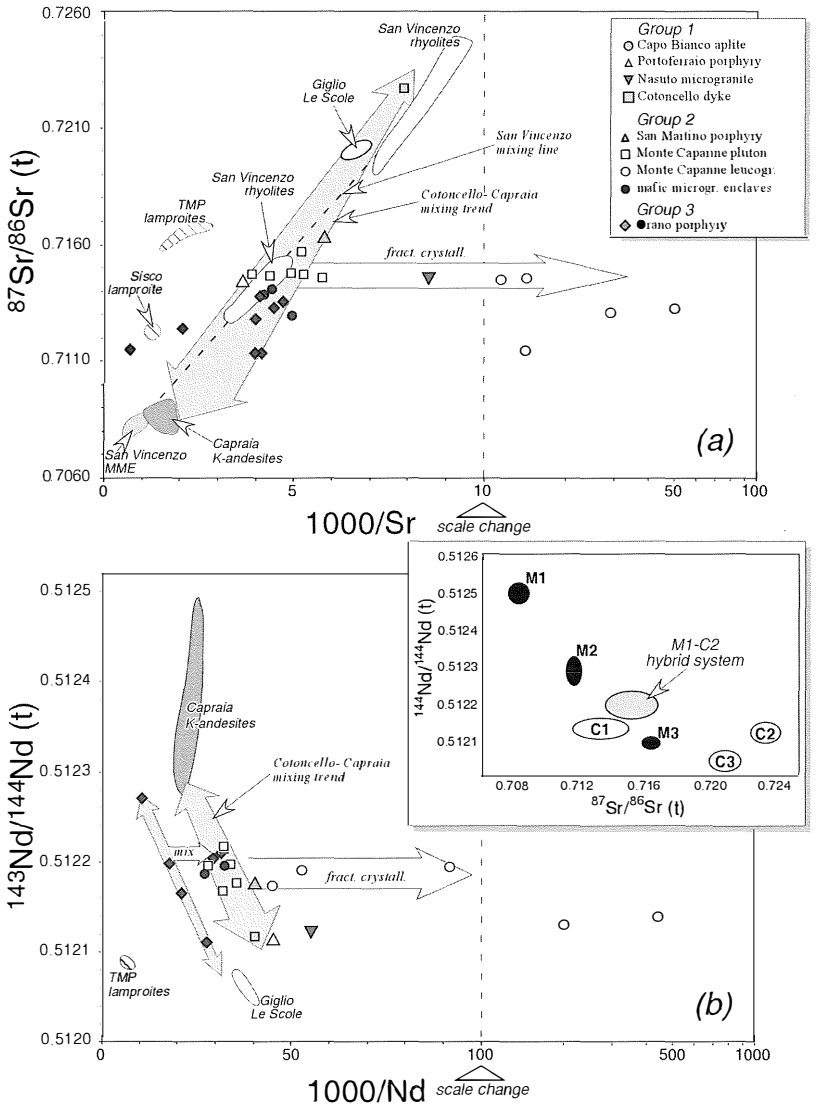

Fig. 13 – (a) $^{87}Sr/^{86}Sr$ vs. 1000/Sr diagram showing possible crustal and mantle-derived components, along with possible mixing trajectories able to produce the cluster of hybrid samples with Sr ca. 200 ppm and $^{87}Sr/^{86}Sr$ ca. 0.7145. Note that a mixing plus fractional crystallisation process with a petrologically likely bulk D_{Sr} close to 1, would lead to the same path as pure mixing. (b) $^{143}Nd/^{144}Nd$ vs. 1000/Nd diagrams showing possible crustal and mantle-derived components, along with possible mixing trajectories able to produce the cluster of hybrid samples. Nd content for Giglio Le Scole extrapolated from La and Ce contents (Westerman *et al.*, 1993). In the inset, ellipses labelled C and M represent crustal and mantle component discussed in the text. C1: crustal source for Capo Bianco aplite. C2: main crustal end-member for hybridism processes in the Tuscan Magmatic Province (exemplified by Cotoncello dyke and some San Vincenzo rhyolites). C3: low $^{143}Nd/^{144}Nd$ crustal source, responsible for deep hybridism of Orano primary melt (exemplified by the Giglio-Le Scole intrusion). M1: main mantle end-member for hybridism processes in the Tuscan Magmatic Province (exemplified by the Capraia K-andesites and the mafic microgranular enclaves from San Vincenzo rhyolites). M2: mantle source for primary Orano magma. M3: mantle source for the lamproites from Tuscan Magmatic Province, not involved in the genesis of Elba magmas. After Dini *et al.* (2002).

component of the Group 2 hybridisation process, and its internal variations are instead linked to shallow level, more or less thorough mingling with a granitic crystal mush, probably during emplacement of the dykes as they passed through the Monte Capanne pluton. In summary, the $^{87}Sr/^{86}Sr$ vs. 1000/Sr and $^{143}Nd/^{144}Nd$ vs. 1000/Nd diagrams illustrate that the most voluminous Group 2 rocks represent a hybridisation trend between Capraia (from M1) and Cotoncello (from C2) end-member magmas. Group 3 Orano rocks represent a mix between a different mantle-derived magma (from M2) having geochemical-isotopic characteristics intermediate between Capraia K-andesites and Tuscan Magmatic Province lamproites, and a different crustal magma (from C3; low $^{143}Nd/^{144}Nd$ isotopic ratio), with additional varieties derived from mingling with Group 2 magmas.

The possible involvement of a magma having lamproitic affinities (i.e. high Rb/Sr) is also suggested by the trace element zoning of K-feldspar megacrysts, which indicate that such a magma could have contributed to the genesis of the Monte Capanne pluton (Gagnevin *et al.*, 2002). Mafic microgranular enclaves displaying unusual $\varepsilon_{Nd}(t)$ could be the result of such interaction with lamproitic magmas. In the same framework, the Group 1 Capo Bianco aplite, Nasuto microgranite and Portoferraio porphyry are crustal melts (from C1) that did not contribute to the main hybridisation processes (Dini *et al.*, 2002).

2.4.3 Summary

The general igneous framework of western-central Elba consists of an acidic laccolith complex intruded by a monzogranitic pluton and a slightly younger swarm of more mafic dykes. Figure 14 schematically summarises the sequence of events that produced the Elba igneous complex (Dini *et al.*, 2002). Capo Bianco aplite melts were produced first, apparently by muscovite dehydration melting of a metapelitic source, identified as C1. As the anatectic process continued, the Nasuto microgranite and Portoferraio porphyry likely originated via biotite dehydration melting of a metagreywacke source. The earliest magmas were produced without any chemical contribution of mantle melts, with melting probably linked to late Miocene lithospheric thinning and decompression, following earlier Oligocene-Miocene orogenic overthickening.

After a period of quiescence, the volumetrically important phase of hybrid magmatism began, involving mantle-derived mafic magmas and peraluminous crustal melts. Mantle magma involved in this phase is never directly represented, being present most prominently as hybrid products preserved in mafic microgranular enclaves. This mantle magma is thought to be similar to the nearby coeval Capraia K-andesites and has been identified as M1. The crustal component of the hybridisation (C2) was derived from a different crustal source than the peraluminous melts of the first phase, and is represented by the Cotoncello dyke. The first voluminous intrusion of the hybrid group, the San Martino porphyry, was produced by incipient melt hybridism. Next came the Monte Capanne pluton from a fully mature hybrid system, with internal facies representing emplacement pulses, and leucogranite dykes derived by fractional crystallisation. Finally, Orano magmas were generated from strongly modified mantle (M2), as products distinctly different than those involved in the earlier main hybridisation process. During their ascent, they were first variably hybridised by mixing with a unique crustal material (C3), and then further modified by capturing material from the Monte Capanne system.

The magma formation processes recorded between ca. 8 and 6.8 Ma by the Elba magmatism, changed from crust-, to hybrid-, to mantle-dominated, as the Apennine fold belt was progressively thinned, heated and intruded by mafic magmas during late Miocene time. Very unusual melts emplaced at the beginning and at the end of the igneous activity were not volumetrically significant and did not contribute to the generation of main hybrid

0.4	low	28	volume (km^3)	24	~ 200	low	very low	low
no	no	no	mafic enclaves	common	common, variable %	no	small	common
1.42	1.29	1.18	average ASI	1.22	1.11	1.15	1.16	0.94 (min)
0.7115-0.7133	0.7146	0.7144	$^{87}Sr/^{86}Sr(t)$	0.7162	0.7145 - 0.7147	0.7145	0.7228	0.7115 (min)
-9.6	-9.9	-10.0	$\varepsilon_{Nd}(t)$	-8.8	-8.1 - -8.8	-8.6	-9.7	-7.0 (max)

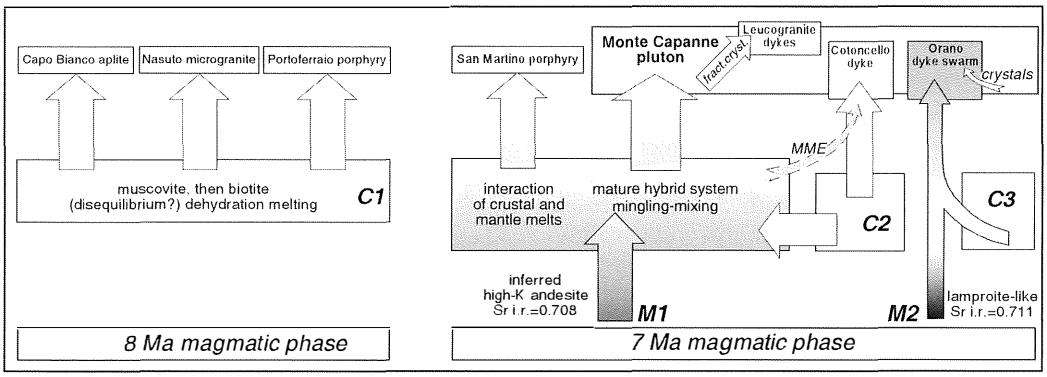

Fig. 14 – Schematic model for the genesis of Elba magmatic products throughout the time. Abbreviations: MME: mafic microgranular enclaves; i.r.: initial isotopic ratio. Modified after Dini *et al.* (2002).

magmas. They do, however, emphasise the highly variable nature of crustal and mantle sources that can be involved, during a short time span, in post-collisional, extension magmatism.

2.5 EMPLACEMENT OF MAGMA

2.5.1 The nested Christmas-tree laccolith complex

Shape and dimension. The main bodies of Capo Bianco aplite, Portoferraio porphyry, and San Martino porphyry have laccolithic shapes (Rocchi *et al.*, 2002): (1) contacts of intrusions share the strike and dip of host flysch bedding (Fig. 15) or tectonic surfaces in the nappe sequence, (2) the sheets clearly taper out at their visible eastern ends (Fig. 15), (3) detailed mapping and cross sections show that the nine main layers have convex-upward roofs and flat or convex-upward floors.

The layers of each unit are connected by small dykes, and major dykes below the overlying sheets are interpreted as feeders (Fig. 3, north of Marciana: SMF). The overall geometry is typical of a multilayered laccolith complex, constituting an outstanding example of shallow-level nested Christmas-tree laccoliths (Corry, 1988; Figs. 3, 16, 17).

These relationships allow determination of the geometric parameters for all the layers (Rocchi *et al.*, 2002; Table 3). Maximum thickness (T) of the nine most significant intrusive layers, along with thicknesses of the intervening and overlying host rock (T_{hr}), were estimated by measurement in cross sections (e.g., Figs. 16 and 17). T values of individual layers vary over an order of magnitude, from 50 to 700 m (Rocchi *et al.*, 2002; Table 3). Intrusion floors were assumed to be roughly circular on the basis of the observation that diameter differences in a single laccolith are generally less than two times (Corry, 1988).

The diameter (L) for each layer was taken as the maximum length of the body as measured on the geological map (Fig. 3). In central Elba, the determined axes strike N-S with lengths between 2.4 and 10 km, whereas in western Elba, they have NE strikes with lengths between 1.6 and 9.3 km (Table 3). The latter was estimated by reconstruction of the

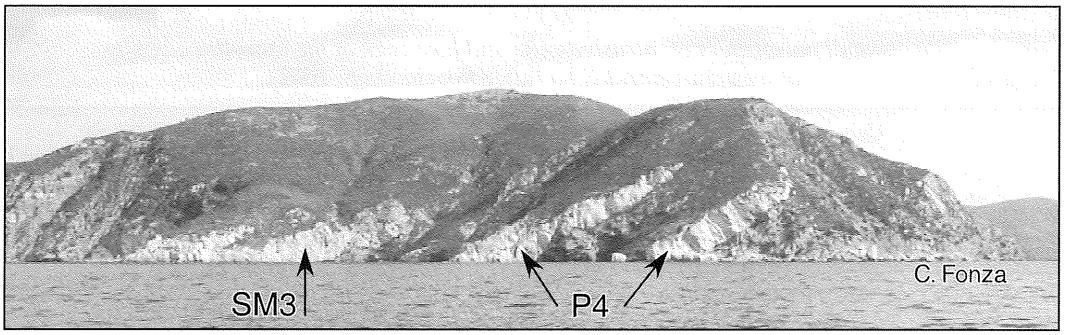

Fig. 15 – View from the south of the WNW-ESE oriented cliff bounding the north of the Gulf of Marina di Campo. SM3 and P4 refer to the laccolith layers as reported in Table 3 and Figure 16.

geometry of layer P3 prior to deformation and truncation by the Monte Capanne pluton, whose intrusion produced mylonitic foliation along its northeast and southwest contacts (Fig. 3). The nine main Elba laccolith layers show diameters varying by nearly an order of magnitude, and they all have large aspect ratios (L/T varies from 12 to 33). Volumes were calculated by approximating the shape of each laccolith layer to a spherical cap with height equal to T and diameter equal to L. The resulting values vary over more than two orders of magnitude, from 0.1 to 24 km^3 (Rocchi *et al.*, 2002; Table 3).

Emplacement depth and structural level. By measuring the overburden from cross sections (plus 800 m, based on an estimate of the present mean erosion rate for Italy of 0.1 mm/yr), the emplacement depths of Elba laccolith layers have been calculated to range from 1.9 to 3.7 km (Rocchi *et al.*, 2002; Table 3). The laccolith layers were emplaced along strong crustal heterogeneities such as thrust surfaces between tectonic complexes, secondary thrusts inside Complex IV, and strong contrasts of strength between arenaceous and argillaceous sequences within the flysch of Complex V. The switch from vertical to horizontal magma movement was not exclusively controlled by reaching the neutral buoyancy level because (1) the magma at its emplacement level had sufficient residual driving pressure to exceed the vertical stress and to lift the overburden and (2) magma batches with the same composition reached depths as different as 1 km. Furthermore, the occurrence of intrusive layers along surfaces of strength anisotropy points out that crustal magma traps (Hogan *et al.*, 1998) played a prominent role in controlling the emplacement level of magma at Elba (Rocchi *et al.*, 2002).

Laccolith growth. On the basis of geological and geophysical reconstruction of the shapes of 125 laccoliths, an empirical power-law relationship linking width (L) and thickness (T) of these intrusive bodies has been proposed (McCaffrey and Petford, 1997). The relationship has the form $L = kT^a$ (where k is a constant and a is the slope of a regression line in a Log-Log plot), suggesting a scale-independent mechanism of growth. A similar scale-invariant distribution of tabular shapes has been documented for 66 plutons (Cruden and McCaffrey, 2001). The mechanism generally acknowledged as most likely for laccolith growth is a two-stage process. First, the magma spreads laterally at the emplacement level with $a < 1$ (the stage of horizontal elongation) until an initial sill is formed having a very high aspect ratio ($L >> T$), and a width nearly equal that of the future intrusion. Then the thin intrusion thickens by dominantly upward inflation and roof lifting along a growth line with $a > 1$. Experiments on vertical growth due to floor subsidence suggest that tabular plutons make room by floor

TABLE 3

Dimensional parameters of intrusive units and host rock of the laccolith complex of western-central Elba (after Rocchi et al., 2002).

	Unit	Layer	Label	Host rock	Intrusive rock layers				
				T_{hr} (m)	T (m)	L (km)	V (km^3)	L/T	Depth (m)
	erosion loss			800					
Central Elba									
	flysch (Complex V)			1100					
	San Martino porphyry	layer 3	SM3		700	8.3	19.1	12	1.9
	flysch (Complex V)			50					
	San Martino porphyry	layer 2	SM2		100	2.4	0.23	24	2.0
	flysch (Complex V)			250					
	San Martino porphyry	layer 1	SM1		200	5.0	1.97	25	2.2
	flysch (Complex V)			400					
	Portoferraio porphyry	layer 4	P4		400	10.0	15.7	25	2.6
	Capo Bianco aplite	layer 2	CB2		≈120	3.5	0.58	29	2.6
Western Elba									
	hornfels (Complex IV)			400					
	Portoferraio porphyry	layer 3	P3		700	9.3	23.9	13	3.1
	Capo Bianco aplite	layer 1	CB1		50	1.6	0.05	32	3.0
	ophiolite (Complex IV)			280					
	Portoferraio porphyry	layer 2	P2		75	≈1.9	0.11	25	3.3
	ophiolite (Complex IV)			210					
	Portoferraio porphyry	layer 1	P1		75	≈2.5	0.18	33	3.7
Totals				2690	2420		62		

Label: label reported on each layer on the geological map (Fig. 1C). T_{hr} = thickness of intervening host rock layers, as determined from cross sections. T = thickness of individual laccolith layers, as determined from cross sections. L = length of individual layers, as measured on the geological map. V = volume of the individual layer, calculated by assuming a laccolith shape equal to the shape of a spherical cap, with maximum thickness = T and diameter = L: $V=\pi T(3(L/2)^2+T^2)/6$. L/T = aspect ratio. Depth: emplacement depth.

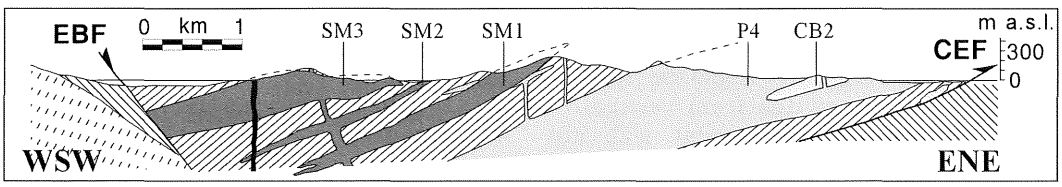

Fig. 16 – Geological section across central Elba Island. Labels of intrusive layers as in Table 3. Modified after Rocchi *et al.* (2002).

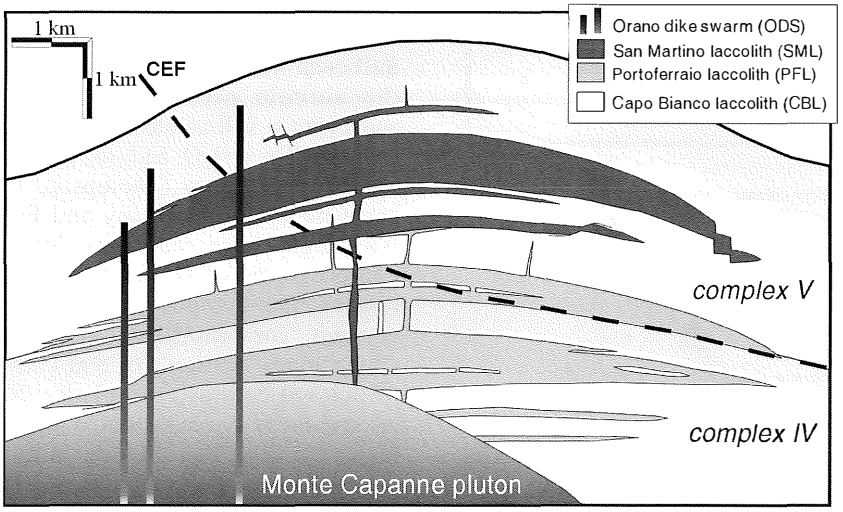

Fig. 17 – Schematic reconstruction of the western Elba Christmas-tree laccolith complex, before tectonic-gravitational decapitation.

depression and grow from an initial thin sill along a line with slope of ca. 6.0 (Cruden and McCaffrey, 2001).

The dimensional parameters collected for the Elba intrusive layers allow testing of these hypotheses. A significant power-law correlation exists between thickness (T) and diameter (L): on a Log-Log plot of T versus L, this correlation results in a linear fit ($r^2 = 0.93$) with the equation $T = (0.026 \pm 0.006)L^{(1.36\pm0.14)}$ (Rocchi *et al.*, 2002; Fig. 18). Owing to the strong coherence of the Elba data set, this scaling curve could replace that of McCaffrey and Petford (1997) to approximate the general power-law for laccolith dimensions. However, each intrusive layer is thought to represent only part of a complete laccolith, and the dimensional parameters of all the layers plot in the horizontal elongation field even though the slope ($a > 1$) of the regression line is typical of vertical self-affine inflation (i.e. intrusions have the same type of shape at different scales, but L and T do not retain the same proportions as the intrusions grow; McCaffrey and Petford, 1997). These observations led us to interpret the collected Elba data as the first record of the occurrence of a vertical inflation stage in laccolith growth (Rocchi *et al.*, 2002).

Finally, the dimensional parameters for each Christmas-tree laccolith as a single unit can be calculated. The basal diameter has been assumed equal to (1) the average diameter or (2) the maximum diameter of the layers composing it. In case (1), the resulting parameters for the Portoferraio and San Martino laccoliths plot on the regression line for pluton dimensions of Cruden and McCaffrey (2001), as do the parameters of the Monte Capanne pluton (Fig. 18). In case (2), the dimensions of Portoferraio and San Martino laccoliths plot on the regression line for laccolith dimensions (Rocchi *et al.*, 2002; Fig. 18). These results indicate that in the case of coalescence of the layers to form three single-layer intrusions, the latter would have dimensions typical of laccoliths or plutons, suggesting that the growth of laccoliths and plutons goes on through the amalgamation of smaller sheet-like bodies. Additionally, it is likely that the multilayer laccoliths at Elba failed coalescence due to an abundance of lithologic and/or tectonic discontinuities that acted as magma traps (Rocchi *et al.*, 2002).

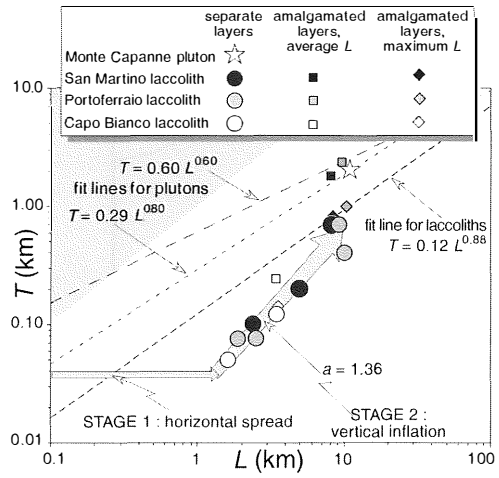

Fig. 18 – Log-Log plot of T vs. L, where T = thickness of individual laccolith layers and L = diameter of individual laccolith layers (Table 3). The regression lines for laccoliths' dimensional parameters (McCaffrey and Petford, 1997), for plutons (McCaffrey and Petford, 1997; Cruden and McCaffrey, 2001), and for Elba laccoliths (Rocchi *et al.*, 2002) are shown. Grey and white areas represent vertical-inflation and horizontal-elongation fields of McCaffrey and Petford (1997), respectively. The inferred dimensions of Monte Capanne pluton are shown. Dimensions for each Christmas-tree laccolith as a whole are calculated as explained in the text. Light grey arrows depict the two-stage development of tabular intrusions reconstructed for Elba laccolith layers, with growth during the second stage along a slope a = 1.36. Modified after Rocchi *et al.* (2002).

The filling time of a pluton like that formed by the amalgamation of San Martino laccolith layers (~22 km^3) can be estimated from the dimensions of its main feeding dyke (~1500 m long x 10–20 m thick, Fig. 1C, north of Marciana: SMF). A magma-ascent rate as low as 3×10^{-3} ms^{-1} would result in filling on a time scale of <10^2 yr (Rocchi *et al.*, 2002).

2.5.2 Monte Capanne pluton and younger dykes

With an exposed diameter of 10 km and an estimated thickness of 2 km on the basis of preliminary magnetic modelling (O. Faggioni, pers. comm.), the total volume of the Monte Capanne pluton is on the order of 80 km, about 4 times that of the San Martino laccolith. Sufficient lithological variation of protoliths in the aureole preserves the reactions (i) andalusite = sillimanite, (ii) talc + forsterite = anthophyllite + H_2O, and (iii) the breakdown of muscovite + quartz (Thompson, 1974; Spear and Cheney, 1989; Tracy and Frost, 1991). Although these reactions depend on the compositions of fluids and solid solution phases, taken together they suggest peak contact metamorphic conditions with temperatures in excess of 600°C at a pressure of 0.1 - 0.2 GPa (Dini *et al.*, 2002). This environment is consistent with palinspastic reconstructions that provide an emplacement depth of 4.5 km (Rocchi *et al.*, 2002).

Faults are mapped along parts of the western and southern contacts of the pluton (Barberi et al, 1967b). Close to the western and northern contacts, the Portoferraio porphyry exhibits a strong mylonitic foliation in the groundmass, with quartz phenocrysts having subgrain boundaries, plagioclase cracks cemented by micrographic quartz plus K-feldspar, and biotite as oriented polycrystalline aggregates. Thermal metamorphism along all these faulted contacts is strong, so movement was significantly less than the thickness of the aureole.

Leucogranite dykes and aplite-pegmatite veins and dykes occur throughout the Monte Capanne pluton, although somewhat more abundantly in the south-eastern half where they have a strong preferred orientation trending NNE (Boccaletti and Papini, 1989). Elsewhere they are either randomly oriented or trend generally perpendicular to the contact. These patterns correspond with those reported for magnetic anisotropy studies which has led to an interpretation that emplacement occurred in an extensional setting (Bouillin, *et al.*, 1993). This pattern of dykes suggests extension in the ESE direction which, along with other evidence, has led to speculation (Jolivet *et al.*, 1994) that pre- to syn-plutonic detachment faulting «opened the door» for the pluton to rise. However, the presence of Monte Capanne hornfels as clasts

in the fault breccia of the Central Elba fault, located some 10 km off to the east of the pluton (see below), as well as clear evidence that unroofing of the pluton occurred following emplacement of the younger Orano dyke swarm, argue for post-emplacement detachment.

About 100 Orano dykes have been mapped, all restricted to the northern portions of western and central Elba and exhibiting a strong E-W orientation (Westerman et al, submitted). They occur up to 50 m thick and 2.5 km long, as well as throughout the section from the lowest exposed levels in western Elba up to the top of the exposed section in central Elba, a total section of several km. Orano magmas interacted with the Monte Capanne magmatic system from which it captured xenocrysts and enclaves, however the dykes sometimes clearly exploited brittle joint structures, testifying to the «solid» character of their host.

2.5.3 Eastern Elba magmatism

In comparison to the Monte Capanne pluton, much less is known about the emplacement of the Porto Azzurro pluton due to its very limited exposure. Recent mapping shows outcrops in a general E-W trending belt about 2 km long, but data from boreholes (Bortolotti et al, 2001). Widespread distribution of contact metamorphic effects attributed to this pluton indicate a broader extent at depth, with emplacement conditions producing peak metamorphism at 600-650°C and about 2 kbar.

2.5.4 Summary

Favourable tectonic conditions at Elba Island have allowed a detailed study of a 5-km thick crustal section including nine intrusive layers of late Miocene age that built up three multilayer Christmas-tree laccoliths. The dimensional parameters of the intrusive layers fit a power-law distribution indicating that, after a likely first stage of horizontal expansion, the layers underwent a second stage of dominantly vertical inflation. The abundantly available crustal magma traps, in many cases, halted the supply of magma which then filled another layer. Laccoliths from Elba can be envisaged as sheet-like intrusions that did not coalesce to form single laccoliths or plutons with dimensions typically observed elsewhere. This in turn suggests that laccoliths and plutons, at least in some cases, grow by amalgamation of smaller sheet-like bodies (Rocchi *et al.*, 2002).

2.6 Tectonic evolution (syn- to post-intrusive)

Large-scale faults subdivide Elba Island into three main zones: western, central and eastern Elba (Fig. 2), and these faults are the key to the reconstruction of the original emplacement geometry of the intrusive complexes. All the intrusive units now located in western and central Elba were emplaced within the tectonic Complexes IV and V, which were piled up above the present western Elba (Fig. 19a; Westerman *et al.*, submitted). Then, shortly after the intrusion sequence was completed, the upper part of the igneous-sedimentary complex was tectonically translated eastward along the Central Elba Fault (Fig. 19b-c), so that the lower part is presently found in western Elba while the upper part is in central Elba (Fig. 19d). The fault gently dips to the west, so that the stratigraphically highest part of the central Elba section occurs at the western edge, where it is cut by the high angle brittle Eastern Border fault. This reconstruction of tectonic dismemberment is based on the following evidence: (i) the igneous layers and their host rocks of central Elba are a complex bounded at its base by a low angle fault, the Central Elba fault, (ii) the footwall mélange of the Central Elba fault (Trevisan, 1950; Perrin, 1975) contains fragments of rocks typical of western Elba outcrops, such as thermally metamorphosed serpentinite and basalt (Marinelli, 1955), garnet- and wollastonite-bearing marble from the Monte Capanne contact aureole (Vom Rath, 1870), tourmaline-free aplite porphyry equivalent to Capo Bianco

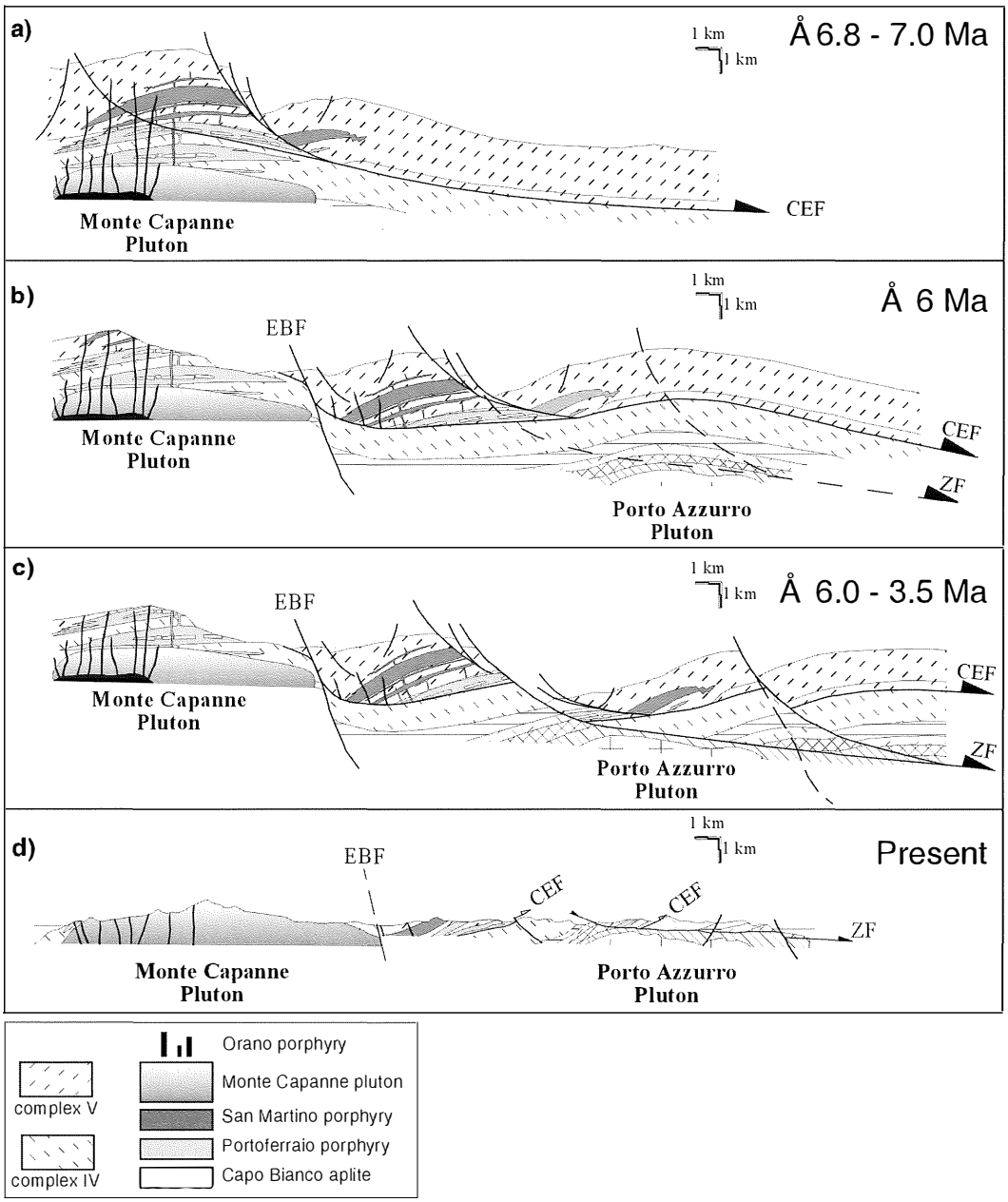

Fig. 19 – Tectonic-gravitational dismemberment of the western Elba intrusive complex (after Westerman *et al.*, submitted).

aplite from western outcrops, and K-feldspar phenocryst-bearing porphyry; (iii) petrographic and geochemical features of the intrusive units cropping out in central Elba fully match those of intrusive units cropping out in western Elba; (iv) in both western and central Elba the Orano dykes crop out only in the northern area and have strong preferred E-W orientation.

After the eastward translation on the Central Elba fault, a «west side up» movement occurred along the Eastern Border fault with a throw of 2 to 3 km. The Eastern Border fault roughly parallels the east side of the Monte Capanne pluton, truncating its contact aureole. The fault has wide variation in attitude, with overall NNE-SSW strike and moderate to steep eastward dip (Figs. 2, 3). For the most part, the fault is marked by a distinct plane separating a western footwall breccia of hornfelsed Complex IV rocks (ophiolitic material and deep marine cover rocks) plus fragments of the Monte Capanne pluton, from an eastern hanging wall breccia made of Complex V flysch and megacrystic San Martino porphyry.

The amount of displacement along the Central Elba fault is constrained by the distance from leading edge of the fault to the pluton's aureole of about 7 to 8 km. The timing of displacement is constrained by the occurrence in the footwall mélange of the Central Elba fault of fragments of the thermometamorphic carapace of the Monte Capanne pluton: the main displacement occurred after the emplacement of Monte Capanne pluton and development of its thermometamorphic aureole, i.e. after 6.8 Ma. However, minor low-angle normal faulting on the Central Elba fault occurred during the emplacement of the oldest (8 Ma) units, because close to the fault, Capo Bianco aplite and Portoferraio porphyry fragments from western Elba show evidence of syn-intrusive deformation. The timing in this scenario is further supported by the occurrence of abundant cobbles and boulders of tourmaline clots-bearing Capo Bianco aplite and Portoferraio porphyry in late Messinian conglomerates on mainland Italy some 50 km to the east (Marinelli *et al.*, 1993). Indeed, Capo Bianco aplite and Portoferraio porphyry layers were concentrated just above the Central Elba Fault, and the most logical mechanism to expose them without exposing the overlying San Martino porphyry units was by raising the Central Elba fault surface as Complex V was translated eastward. The rate of displacement is constrained by the time between beginning of the main movement along Central Elba fault (6.8 Ma) and the time cobbles were produced and deposited (late Messinian), that is about 2 myr. Allowing for erosion and transport, a maximum estimate for the time available for movement on Central Elba fault could be about 1.5 myr. Thus the eastward translation of about 7-8 km occurred at an average rate of about 5-6 mm/yr, a movement rate consistent with the typical rates of tectonic movements associated with magma emplacement.

A similar sequence of events occurred also for the tectonic evolution and pluton exhumation in eastern Elba (Keller and Pialli, 1990; Pertusati *et al.*, 1993). The common history for both regions began initially with dominantly, sub-horizontal movement on a low-angle detachment fault with top-to-the east sense of shear (Central Elba and Zuccale faults), translated the overlying rocks eastward while trimming out part of the contact aureole of the pluton with which it is associated. Then, high-angle structures were activated at the eastern edge of the pluton, i.e. the Eastern Border fault east of the Monte Capanne pluton, and off-shore faults east of the Porto Azzurro pluton. In this picture, pluton emplacement occurred before the main faulting, and promoted its activation. This inference challenges the hypotheses of pull-apart opening (Bouillin *et al.*, 1993) or top-to-the-east shear above the pluton (Jolivet *et al.*, 1998; Daniel and Jolivet, 1995; Rossetti *et al.*, 2000) yielding room to the magma and controlling the level of emplacement of the Monte Capanne and Porto Azzurro plutons.

The eastward displacement of the upper part of the complex is at least partly linked to gravitational instability. Indeed, in a time span of about 1 myr, a 2700 m thick

tectonostratigraphic section was inflated by addition of a total of 2400 m of laccolithic intrusions, leading to a total thickness for the new section of about 5000 m. A dome with a 10 km diameter and a height of 2.5 km, was produced with a surface slope of about 25° (assuming originally flat surface). The emplacement of Monte Capanne pluton led to the oversteepening of the dome and triggered the main eastward displacement of the upper section. Once significant movement began, transfer of the load from above Monte Capanne towards central Elba promoted movement on the east-dipping Eastern Border fault as the unloaded pluton rose and the thickened central Elba section subsided. Final movement on the Eastern Border fault took place entirely in the brittle regime, truncating the Central Elba fault which has since been eroded in western Elba and lies almost completely buried below central Elba.

This paper is based on the following works:

A. DINI, F. INNOCENTI, S. ROCCHI, S. TONARINI and D.S. WESTERMAN – *The magmatic evolution of the laccolith-pluton-dyke complex of the Elba Island, Italy*, in Geological Magazine **139,** 257-279, 2002.

S. ROCCHI, D.S. WESTERMAN, A. DINI, F. INNOCENTI and S. TONARINI – *Two-stage laccolith growth at Elba Island (Italy)*, in Geology **30,** 983-986, 2002.

D.S. WESTERMAN, A. DINI, F. INNOCENTI and S. ROCCHI – *Rise and fall of a nested Christmas-tree laccolith complex, Elba Island, Italy*, submitted for publication in Geological Society Special Publication, N. Petford editor.